Bone 167 (2023) 116615

Contents lists available at ScienceDirect

Bone

journal homepage: www.elsevier.com/locate/bone

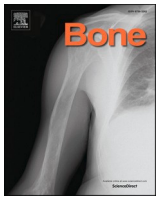

Full Length Article

Osteopetrosis: Gene-based nosology and significance Dysosteosclerosis

Serap Turan *

Pediatric Endocrinology and Diabetes, Marmara University School of Medicine, Istanbul, Turkey

ARTICLE INFO

Keywords:
Dysosteosclerosis
Bone fractures
Osteopetrosis
Osteosclerosis
Osteopenia
Optic atrophy
Jaw necrosis
Metaphyseal osteosclerosis
Osteosclerotic metaphyseal dysplasia
Pyle disease
Brain abnormalities
Neurodegeneration
Dementia
Leukoencephalopathy
SLC29A3
TNFRSF11A
TCIRG1
LRRK1
CSF1R
TNFSF11

ABSTRACT

Dysosteosclerosis (DSS) refers to skeletal dysplasias that radiographically feature focal appendicular osteosclerosis with variable platyspondyly. Genetic heterogeneity is increasingly reported for the DSS phenotype and now involves mutations of *SLC29A3*, *TNFRSF11A*, *TCIRG1*, *LRRK1*, and *CSF1R*. Typical radiological findings are widened radiolucent long bones with thin cortices yet dense irregular metaphyses, flattened vertebral bodies, dense ribs, and multiple fractures. However, the radiographic features of DSS evolve, and the metaphyseal and/or appendicular osteosclerosis variably fades with increasing patient age, likely due to some residual osteoclast function. Fractures are the principal presentation of DSS, and may even occur in infancy with *SLC29A3*-associated DSS. Cranial base sclerosis can lead to cranial nerve palsies such as optic atrophy, and may be the initial presentation, though not observed with *SLC29A3*-associated DSS. Gene-specific extra-skeletal features can be the main complication in some forms of DSS such as *CSF1R*- associated DSS. Further genetic heterogeneity is likely, especially for X-linked recessive DSS and cases currently with an unknown genetic defect. Distinguishing DSS can be challenging due to variable clinical and radiological features and an evolving phenotype. However, defining the DSS phenotype is important for predicting complications, prognosis, and instituting appropriate health surveillance and treatment.

1. Introduction

Dysosteosclerosis (DSS) is regarded as a skeletal dysplasia (OMIM % 224,300) [1] and was first described in 1934 by Ellis [2] who described 2 brothers from consanguineous English parents and, considered it osteopetrosis (OPT). In 1968, Spranger and colleagues described the disease as a distinct entity [3]. Spranger described the radiological features in a 12-year-old boy as widened radiolucent long bones with thin cortices ends to the dense irregular metaphyses, flattened vertebral bodies, dense ribs, and multiple fractures [3]. DSS is categorized as an osteosclerotic disease, rather than a nonhomogeneous osteosclerosis (i.e. coexistence of radiolucent bones together with dense bones), to differentiate DSS from OPT. Nevertheless, DSS is classified as an OPT-related disorder by the International Skeletal Dysplasia Registry [4] in line with the first report of Ellis [2]. Clinical features of DSS are recurrent fractures, short stature, failure of tooth eruption, and, sometimes optic atrophy and other cranial nerve palsies, developmental delay, and skin changes [2,3,5–11]. As radiological and clinical findings are variable (See below) making a diagnosis can be challenging. Clinical and radiological criteria for DSS are shown in Table 1.

Since DSS mimics the clinical and radiological findings of OPT to a degree, candidate gene defects that compromise osteoclast function and/or osteoclastogenesis may be causal. In 2010, Whyte et al. reported an American girl of Turkish heritage with DSS, but with histological features that suggested this was an "osteoclast-poor" form of OPT with a skeletal resorption defect and absence of osteoclasts in bone biopsy [5]. In 2012, delineation of the genetic basis for DSS began with detecting compound heterozygous loss-of-function mutations (c.607 T > C, p.

* Marmara University School of Medicine, Department of Paediatric Endocrinology and Diabetes, Fevzi Cakmak Mh. Muhsin Yazicioglu Cd. No 41. 34899, Ustkaynarca/Pendik, Istanbul, Turkey.
E-mail address: serap.turan@marmara.edu.tr.

https://doi.org/10.1016/j.bone.2022.116615
Received 3 July 2022; Received in revised form 9 November 2022; Accepted 12 November 2022
Available online 17 November 2022

Table 1
Diagnostic criteria for DSS.

Clinical criteria	Radiological criteria
Exclusion	**Exclusion**
1. The finding of persistent bone marrow medullary space occupation a. Pancytopenia b. Extramedullary hematopoiesis c. Indication of bone marrow transplantation for bone marrow failure	Diffuse osteosclerosis
Inclusion	**Inclusion**
Optic atrophy or cranial nerve palsies −/+ and osteonecrosis or osteomyelitis of jaw can be seen	***Early Childhood:*** Widened metaphyses, Metaphyseal/epiphyseal osteosclerosis with submetaphyseal/diaphyseal radiolucency and thin cortical bones. Platyspondyly −/+, sandwich vertebrate −/+ ***Late Childhood-Adult:*** Focal sclerosis of under-modeled tubular bones with radiolucent diaphysis and thin cortices. Platyspondyly −/+, sandwich vertebrate −/+ Relatively preserved axial skeleton osteosclerosis in comparison with appendicular skeleton. ***Adulthood:*** Under-modeled tubular bones with radiolucent diaphysis and thin cortices, irregular focal sclerosis of long bones. Sclerotic band of the closed epiphyseal plate. Platyspondyly −/+, sandwich vertebrate −/+

Ser203Pro; and c.1157G > A, p.Arg386Gln) of the *SLC29A3* gene (OMIM*612373) in this girl and, also homozygous *SLC29A3* (c.1346C > G, p.Thr449Arg) mutation in another girl with DSS [6]. Since then, variants in two genes were identified as a cause of the DSS phenotype with autosomal recessive OPT (AR-OPT) (OMIM # 612301 and # 259700) [1,12,13]; i.e., tumor necrosis factor receptor superfamily member 11A (*TNFRSF11A*) that encodes "receptor activator of NF-κB" (RANK), and "T-cell immune regulator 1" (*TCIRG1*) that encodes a component of the vacuolar proton (H+) pump in OCs and gastric mucosa [14,15]. Additionally, homozygous mutations in the gene encoding "leucine rich repeat kinase 1" (*LRRK1*) (OMIM *610986) and bi-allelic mutation of "colony-stimulating factor 1 receptor" (*CSF1R*) (OMIM *164770) have been identified in the etiology of "osteosclerotic metaphyseal dysplasia" (OMD) which has overlapping features of the clinical and radiological findings of DSS (OMIM # 615198), and, "DSS-Pyle disease" (DSS-PD) also called "brain abnormalities, neurodegeneration, and dysosteosclerosis" (BANDDOS: OMIM # 618476), respectively [16,17].

Before the delineation of the genetic basis of DSS, 22 cases were reported as DSS including the first case of Ellis in the literature [2,3,5,7–10,18–30]. Of these only 15 patients full-filled the criteria of DSS [2,3,5,7–10,18–25] after excluding 5 cases with a phenotype matching OPT [26–28] and two other patients with a sclerosing bone dysplasia [29,30]. Several cases have been reported more than once [2,3,7,11,31–33]. After the first genetic report of DSS, among 26 patients with genetic results; *SLC29A3* defects were found in eight [6,13,34–37], *TNFRSF11A* in five [12,38–41], *TCIRG1* in two [13], and *CSF1R* in eleven [17,42,43] (Table 2). Two patients with *TNFRSF11A* had generalized osteosclerosis compatible with OPT [39,40]. Additionally, among seventeen individuals with OMD phenotype, ten patients had *LRRK1* mutations [16,44–52]. In summary, a total of 56 patients with similar bone phenotypes excluding individuals with OPT phenotype have been reported.

2. Clinical findings

Although clinical and radiological findings are almost always described in children, patients defined in adulthood and/or with long-term follow-up provide information about the natural history of the disease [7,11,33,37,38,50]. The longest and most detailed followed DSS patient is a 44 years of age male reported from 15 months [7,11,33] in whom no genetic etiology has been detected including *SLC29A3*, *TNFRSF11A*, and *TCIRG1* [53]. Additionally, a 59-year-old man with homozygous *TNFRSF11A* mutation [38], a 34-year-old man with homozygous *LRRK1* mutation [50], and a 23-year-old woman with homozygous *SLC29A3* mutation [37] are the oldest reported individuals with a genetic etiology.

Clinical features were mostly dependent on the degree and extend of osteosclerosis ranging from cranial nerve palsies to fractures and short stature, but no findings related to bone marrow failure. In some patients with a DSS phenotype there were distinctive findings related to the underlying genetic etiology.

In the following sections, the clinical and radiological features are reviewed for the cases where no genetic mutation has been identified, and then the gene-specific features are explored for those with known genetic mutations.

2.1. Bone fractures

Fractures are the clinical finding usually leading to diagnosis, and, starting from early childhood. Long bone fractures affecting the lower extremity are the most frequent [3,11], yet, recurrent fractures of the metacarpal and phalangeal bones have also been reported [7,10,11]. Fractures usually occur through osteosclerotic bones or at the junction of radiolucent and dense bone in childhood [5,6,12,37], while in later ages, under-modeled osteopenic long bones may also predispose to fractures [11,37,38,50], indicating poor bone quality in both osteosclerotic and osteopenic bone in DSS.

Fractures are the most common presenting findings in patients with *SLC29A3* mutations from early infancy [5,6,34,35,37]. Recurrent fractures in lower and upper extremities from the first two years of life are the main feature, as they have the highest number of fractures (i.e. 7 fractures up to age 5) [5,6,34,35,37] in comparison to DSSs related to other genes [12,13,16,17,37–42,48–50]. Almost all cases with *SLC29A3* defects present with fractures, while fractures are detected in 60 % of the *LRRK1* [16,48–51] and *TNFRSF11A* defects [12,37,38,40], and, 25 % of *CSF1R* defects [17,43]. Recurrent fractures are also a primary presentation of those with *LRRK1* mutations but fractures may occur in later in life with an age of the first fracture 2 to 25 years [48–51]. Similarly, fractures associated with *TNFRSF11A* defects manifest at older ages i.e. during adolescence [12,37,38]. Although fractures do not occur in all cases, when a fracture presents it can become a significant complication due to subsequent skeletal deformity and/or requirement for multiple surgeries [12,37,38]. By contrast, fractures are not the main presentation of *CSF1R*-associated DSS - only one patient with a coccyx fracture at age 5 years [17] and a long bone fracture in an adolescent boy [43] have been detected. It is possible that the rarity of fractures in similar bony features could be related to primary neurological deterioration and immobility of the patient with DSS-Pyle phenotype.

2.2. Growth features

Short stature is a constant finding in DSS, but prenatal growth is not affected and, birth weight and length are usually normal [8–10]. Linear growth is affected after birth and, short stature is detected during childhood [7–10]. In *SLC29A3* cases there is a normal birth length and, short stature from early childhood [5,6,13,36,37]. Short stature is also detected in almost all cases with *TNFRSF11A*-associated and *TCIRG*-associated cases and half of the *LRRK1*-associated cases, while no information regarding prenatal or early postnatal growth exists (Table 2).

Table 2
Demographic, clinical and radiological features of DSS according to genetic etiology.

Genetic defect (#Patient/#Family)	*SLCA29A3* (8/8) [6,13,34–37]	*TNFRSF11A* (5/5) [12,38–41]	*TCIRG1* (2/1) [13]	*CSF1R* (11/5) [17,42,43]	*LRRK1* (10/6) [16,48–52]
Mutations	c.303_320dup (Hom), p.S203P/p.R386Q, p.R386Q(Hom), p.P391H (Hom), p.T449R (Hom), p.Y428*(Hom)	[a]c.616 + 3A > G (Hom), [a]c.784G > T (Hom), [a]c.414_427 + 7del/c.1664del, p.R129C (Hom), p.R7Cfs*172 (Hom)	c.117 + 4A > C/p.A796fs*34	p.P132L/p.Q481*, p.S620delins40/p.K27del, p.P658Sfs*24 (Hom), [a]c.2763 + 1G > T (Hom), p.Q481* (Het)	p.A34Pfs*33 (Hom), p.E929* (Hom), p.E1980Afs*66 (Hom), p.A1991fs*31 (Hom), p.T1989G1990del (Hom), Not given (Hom)
Sex ratio	F(8)/M(0)	F(3)/M(2)	F(1)/M(1)	F(7)/M(4)	F(4)/M(4)/ND(2)
Ethnicity (Families)	Turkish(6), ND(1), Cameroonian (1)	Turkish(3), Japanese(1), British (1)	Indian(2)	Brazilian(1), Japanese(1), [b]Chaldean(2 + 3), Turkish (3), American (1)	Iranian (1), Indian (2), Moroccan(1), Bulgarian (1), Palestinian (3), British (2)?
Short Stature	75 %	80 %	100 %	25 %	40 %
Skin changes	50 %	0 %	0 %	0 %	0 %
Optic atrophy	0 %	80 %	0 %	25 %	30 %
Macrocephaly	12.2 %	[c]20 %	0 %	25 %	30 %
Developmental delay	12 %	40 %	50 %	100 %	30 %
Convulsions	0 %	[d]20 %	0 %	37.5 %	0 %
Recurrent Infections	37.5 %	[e]40 %–20 %	0 %	0 %	[e]30 %
Anemia/pancytopenia	25 %	20 %	0 %	0 %	20 %
Hepatosplenomegaly	0 %	20 %	0 %	0 %	10 %
Hypercalcemia	12 %	0 %	0 %	0 %	0 %
Dental problems	42 %	60 %	0 %	0 %	60 %
Fractures	87.5 %	60 %	50 %	25 %	60 %
Delayed fracture healing	25 %	0 %	0 %	0 %	0 %
Radiographs					
Osteosclerosis of calvaria	87.5 %	100 %	100 %	87.5 %	30 %
Platyspondyly	87.5 %	100 % (Mild 40 %)	100 %	87.5 %	10 %
Vertebral sclerosis	87.5 %	100 %	100 %	50 %	70 %
Rib Sclerosis/Thickening	87.5 %	100 %	100 %	37.5 %	50 %
Pelvis-peripheral sclerosis	62.5 %	60 %–40 % (Diffuse)	ND	62.5 %	40 %
Metaphyseal sclerosis	87.5 %	40 %	100 %	12.5 %	60 %
Erlenmeyer Flask deformity/Undertubulation	75 %	80 %	100 %	100 %	70 % (Mild)
Diaphyseal osteopenia and thin cortices	37.5 %	40 %	0 %	100 %	30 %
Diaphyseal diffuse sclerosis	0 %	60 %	100 %	0 %	0 %
Diaphyseal focal sclerosis	37.5 %	40 %	0 %	100 %	70 %
Changing sclerosis with age	62.5 %	ND	ND	ND	20 %
Normal bones of hand &forearm bones	0 %	40 %-Mild	0 %	0 %	0 %
Others	Delayed closure of fontanelle (2) Melanocytic nevi (1)	Craniosynostosis, Hydrocephalus		Brain malformations, Calcifying leukoencephalopathy, Epilepsy	Acroosteolysis

[a] Splice donor site mutations.
[b] The clinical information of 2 patients was available for the evaluation.
[c] Intracranial extramedullary hematopoiesis.
[d] Hypocalcemic.
[e] Osteomyelitis.

In *CSF1R* defects, neither prenatal nor postnatal growth is affected, and only 25 % of the patients had short stature [17,42]. Thus, fetal growth is mostly normal in patients with DSS, and depending on the etiology, postnatal growth is compromised in infancy and childhood leading to short adult height. Final height is disproportionately short due to a short trunk in spite of long bone fractures while body proportions are normal during childhood [37]. Changes in body proportion might be explained by progressive loss of vertebral height or more severely affected vertebral growth rather than tubular bone growth. Thus, as body proportions evolve with age in DSS, regular evaluation of body proportions is required during follow-up. We showed that two patients, one *TNFRSF11A*-associated DSS and, one *SLC29A3*-associated DSS, had short-trunk dwarfism with spared arm span [37]. Short extremities were also described in historical and X-linked inherited cases [3,10] and in one adult individual with *CSF1R* defects among the genetically proven cases [17]. Since body proportions had been evaluated in only very few cases, further information is required to explore the effect of specific genes on body proportions. Puberty is an important time for growth and body proportion changes. While no data exists on pubertal growth for DSS, delayed puberty was detected in one historical patient [7], and the pubertal delay has not been described in any of the cases with genetic mutations.

2.3. Cranial nerve palsies

Optic atrophy is variably detected in DSS, but if present can be the earliest presenting clinical feature. Optic atrophy manifests as abnormal eye movement and blindness in early infancy [2,7,8,10]. Cranial nerve

palsies leading to blindness, deafness, and facial paralysis can also be part of the clinic picture depending on the degree of cranial bone osteosclerosis [2,7,8,10,11]. However, cranial nerve palsies and optic atrophy have not been described in association with *SLC29A3* mutations and *TCIRG1* mutations. Optic atrophy is quite common in *TNFRSF11A* defects even after excluding the patients with OPT phenotype and at least half of individuals with *TNFRSF11A*-associated DSS have this complication. Optic atrophy or optic canal narrowing is occasionally detected in those with *CSF1R* and *LRRK1* mutations [17,51] (Table 2).

2.4. Dental complications

Teeth problems in DSS are very common and start from early childhood and include problems with tooth eruption, delayed or premature loss of primary dentition, dentition embedded into the gum, oligodontia, frequent caries, easily broken teeth, and discoloration [7–11,18]. In older ages, osteomyelitis and osteonecrosis of the mandible are the main cause of morbidity [28].

In genetically proven cases, dental problems are most commonly detected in cases with *TNFRSF11A* [12,38,40] and *LRRK1* mutations [48,50–52], and also with *SLC29A3* mutations [13,37], but to date not with *CSF1R* and *TCIRG1* mutations (Table 2). Chronic osteomyelitis of the jaw starting from age of 51 years was reported in the oldest reported case with DSS who had *TNFRSF11A* mutation (c.784G > T) [38], while osteomyelitis of the mandible was detected in 5.3 years girl with *TNFRSF11A* mutation (p.R129C) who had OPT phenotype [40]. However, osteomyelitis of the jaw bone occurs in younger ages in patients with *LRRK1*-associated DSS, such as; recurrent osteomyelitis of the jaw beginning from eight and seven years of age respectively in two different patients [51,52]. Although intrinsic dental problems and/or poor dental hygiene could be the reason for osteomyelitis, the degree of osteosclerosis or severity of osteoclast dysfunction could increase the likelihood of dental problems and osteomyelitis.

2.5. Neurodevelopmental problems

In DSS, macrocephaly (head circumference $\geq +2$ SD or 97th centile) has been detected in some historical cases and genetically proven patients [8–10]. Thus macrocephaly, is a feature of DSS and is most commonly detected in *CSF1R* and *LRKK1* defects [16,17,42]. Only one case with *SLC29A3* defect [5,6] was found to have macrocephaly and none in *TNFRSF11A* and *TCIRG1* defects. Intracranial extramedullary hematopoiesis was the likely cause of macrocephaly in one DSS/OPT case with homozygous *TNFRSF11A* mutation (p.R129C) [40]. Macrocephaly is usually detected at birth and normalized at older ages [8,9,17]. Neurodevelopmental delay and/or deterioration of neurological function and convulsions are the characteristic features of the *CSF1R* defects related to brain malformation with calcifying leukoencephalopathy [17,42,43]. The phenotypical features of two historical cases are compatible with *CSF1R* defects with developmental delay, macrocephaly, convulsions, and intracranial calcification [8,9]. Before the cranial imaging era, several cases of developmental delay and seizures were also reported [2,10,19,31].

2.6. Recurrent infections

Recurrent respiratory tract infections and some requiring adenotonsillectomy were reported in historical cases [11,31]. Among the genetically proven cases, individuals with *SLC29A3* mutation were shown to be prone to recurrent respiratory tract infections [5,6,36], and one patient with *TNFRSF11A* homozygous mutation had recurrent lower respiratory infections requiring hospitalization, and, died due to sepsis at 26 months of age [41]. Although immunoglobulin levels were not given for this latter case, *TNFRSF11A*-related OPT is associated with recurrent infection and hypogammaglobulinemia [14], and, the clinical and radiological features of this case may have been more compatible with OPT.

We reported an individual with no known genetic etiology with recurrent upper and lower respiratory tract infections requiring adenotonsillectomy [37]. This patient also had severe neurodevelopmental delay without any accompanying seizures [37].

2.7. Skin findings

Skin manifestations of DSS have been described as violet, greyish, or dark rose-colored macular lesions with varying in size, appearance, and consistency [2,10,31]. Roy et al. [24] reported a 12-year-old girl with the clinical and radiological characteristics of DSS, and cutaneous findings of small, depressed skin plaques, with slight rarefaction of the elastic layer of the dermis histologically. Similarly, Ellis and Field [2,31] described the skin changes as macular atrophy over the front of the chest and upper part of the abdomen. Wrinkling and dryness of hand, thighs, and calves and orange color change of palm have been reported in another case with mental retardation and optic atrophy [8].

Among the genetically proven cases, maculopapular skin changes were described in a case with *SLC29A3* mutation [5]. Hypertrichosis is also observed [36,37] and is likely a clinical feature of *SLC29A3*-associated DSS. Melanocytic nevi were documented in a case with *SLC29A3*-associated DSS [36]. In contrast to the historical cases with skin changes, the patients with *SLC29A3* defects did not have mental retardation or optic atrophy [2,8–10,31]. It is possible that skin findings of the later reported cases with neurological problems i.e. *CSF1R* defects, remained undocumented due to the severity of neurological findings.

2.8. Hematological features

The absence of persistent cytopenia or bone marrow failure should be the primary clinical criteria used to differentiate DSS from OPT, which could be a rule of thumb for DSS (Table 1). Anemia, thrombocytopenia, bone marrow failure, and related extramedullary erythropoiesis are not the features of DSS, but rather OPT.

Transient anemia was found just in two cases with *SLC29A3*-associated DSS, one case with *LRRK1*-associated DSS, and one with an unknown genetic cause [13,19,37,50]. However, among the reported five *TNFRSF11A*-associated DSS cases; one had anemia, thrombocytopenia, and extramedullary hematopoiesis, thus is case is better described as OPT not DSS [40]. Another case required hematopoietic stem cell transplantation (HSCT) at age 3.1 [39], indicating a more severe phenotype, and was likely OPT rather than DSS. Additionally, radiological findings in both cases showed rather diffuse osteosclerosis which was more consistent with OPT.

3. Radiological findings

DSS is diagnosed mainly by radiological findings in combination with the clinical findings/criteria related primarily to bone resorption defects. Radiological findings of DSS are characterized by focal osteosclerosis of undertubulated long bones, and mostly undertubulated short bones of the hand, accompanied by thin cortices and axial osteosclerosis with or without flattened vertebral bodies. Important distinguishing features are that diffuse osteosclerosis is not a finding of DSS, but osteopenia or radiolucent bones accompanying osteosclerosis are suggestive of DSS (Table 1). However, the shape of the long bones is preserved except for Erlenmeyer flask deformity or undertubulation. The radiological features of DSS show variation from one person to another, and also the radiological features evolve with age. The evolving pattern of radiological features can be observed from radiographs taken longitudinally from the same patient [5,7,11,31,36,37].

One of the longest followed cases was a 44-year-old man who had radiological examinations from 20 months of age. In this patient, the most striking changes were observed up to age 15 years but there was no distinctive change other than decreasing osteosclerosis during

adulthood [7,11]. Initially, during early childhood, mild undertubulation with expanded osteosclerotic metaphyses and subsequent radiolucency up to the mid diaphysis were observed in long bones and short bones of hands [7]. Up to the age of 5.5 years, osteosclerosis expanded and became patchy in broadened submetaphyseal region [7]. In the late adolescent period, osteosclerosis faded, and the prominent finding was radiolucent undertubulated long bones with thin cortices, and, marginal sclerosis at the metaphysis [7]. These findings were consistent through adulthood, but vertebral and axial skeleton sclerosis decreased with age [11]. Furthermore, the vertebral bodies were small and ovoid at age 20 months and became flattened with irregular end plates and diffuse sclerosis at age 15 years [7], but diffuse osteopenia with end plate sclerosis and multiple compression fractures were evident at age 44 years [11]. A short and wide femoral neck was a constant feature at all ages [7,11]. Cranial bones showed diffuse sclerosis of the mandible, maxilla, mastoid, skull, and skull base with unerupted teeth and hypoplastic sinuses. No genetic etiology was detected in the *SLC29A3*, *TNFRSF11A,* and *TCIRG1* genes in this patient [53].

3.1. SLCA29A3-associated DSS

In cases with biallelic *SLCA29A3* mutations; widened metaphysis, metaphyseal and epiphyseal osteosclerosis with radiolucent submetaphyseal diaphysis are the most distinguishable radiological finding in early childhood [5,6,35–37]. Metaphyseal osteosclerosis seems to expand through diaphysis with age/growth, most likely related to remaining unresorbed calcified cartilage embedded within the diaphysis and the sclerotic metaphysis continues to expand with growth. Metaphyseal/diaphyseal osteosclerosis becomes patchy with time as a result of bone resorption depending on the remaining osteoclast function [5,6,37]. This resorption defect during growth leaves under-modeled long bones leading to Erlenmeyer flask deformity. However, after epiphyseal fusion, osteopenia rather than sclerosis seems to be the dominant bone phenotype with fading of interlacing sclerosis [37] (Fig. 1). The extent of expansion of osteosclerosis or the age at the fading of osteosclerosis are variable, even with the same genetic mutation [13,36,37]. Therefore, metaphyseal osteosclerosis and/or patchy sclerosis of long bones are the most remarkable finding in *SLC29A3* defects, and, osteopenia with or without focal sclerosis and/or under-modeled long bones can be the only findings in later ages.

Moreover, the axial skeleton shows more consistent osteosclerosis than long bones, while the resolution of osteosclerosis with age especially during adulthood is likely [36,37]. Vertebrae demonstrate endplate sclerosis with osteopenia and varying degree of platyspondyly which may also show variation with age [5,36,37]. The ribs can be broad and fragile [5,6,34]. Osteosclerosis of the skull base and periorbital region, and, obliteration of cranial sinuses are observed in the majority of the cases [13,37], but, diffuse sclerosis of cranial bones is rare [13]. Peripheral sclerosis of pelvic bones giving a bone-in-bone impression is unique to DSS [5,6,36,37], and resolution of peripheral sclerosis is also observed with age [36,37] (Fig. 1). The femoral neck can be short and mildly widened or normal probably related to the severity of osteosclerosis [5,6,13,36,37]. Radiological features of DSS according to specific genetic defect is given in Table 2.

3.2. TNFRSF11A-associated DSS

When the radiographs of the patients with *TNFRSF11A*-associated DSS were evaluated, only two patients had a phenotype fitting DSS with undertubulated radiolucent long bones and remarkable axial

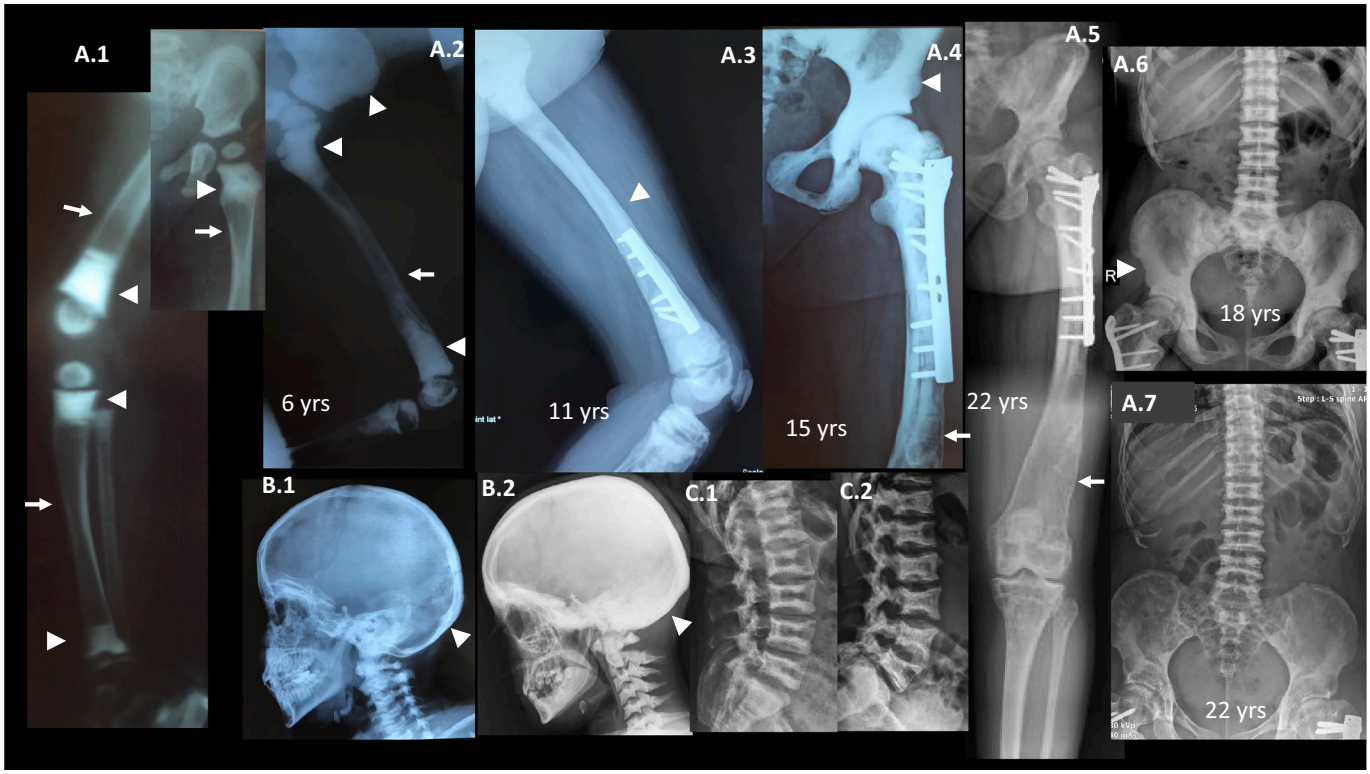

Fig. 1. A.1 to A.7 show the evolution of radiological findings in *SLC29A3*-associated DSS: Lower extremities show dense metaphyseal and epiphyseal sclerosis in early childhood (A.1). At ages 6 and 11 years, osteosclerosis is more diffuse (A2, A3). At age 15 years, pelvic bones give the impression of a bone-in-bone appearance with a more lucent center and dense osteosclerosis in the pelvic bone and femoral heads (A4). At age 22 years, the findings are improved, including the pelvis, vertebrae, and lower extremities showing decreased osteosclerosis, tubulation errors with radiolucent diaphysis, and thin cortices (A5-A7). B and C illustrate the difference between the *SLC29A3*-associated DSS (B.1, C.1) and *TNFRSF11A*-associated DSS (B.2, C.2) with more intense osteosclerosis and thickening of cranial bones in *TNFRSF11A*-associated DSS. Arrowheads and arrows point out osteosclerosis, and radiolucent bone, respectively.

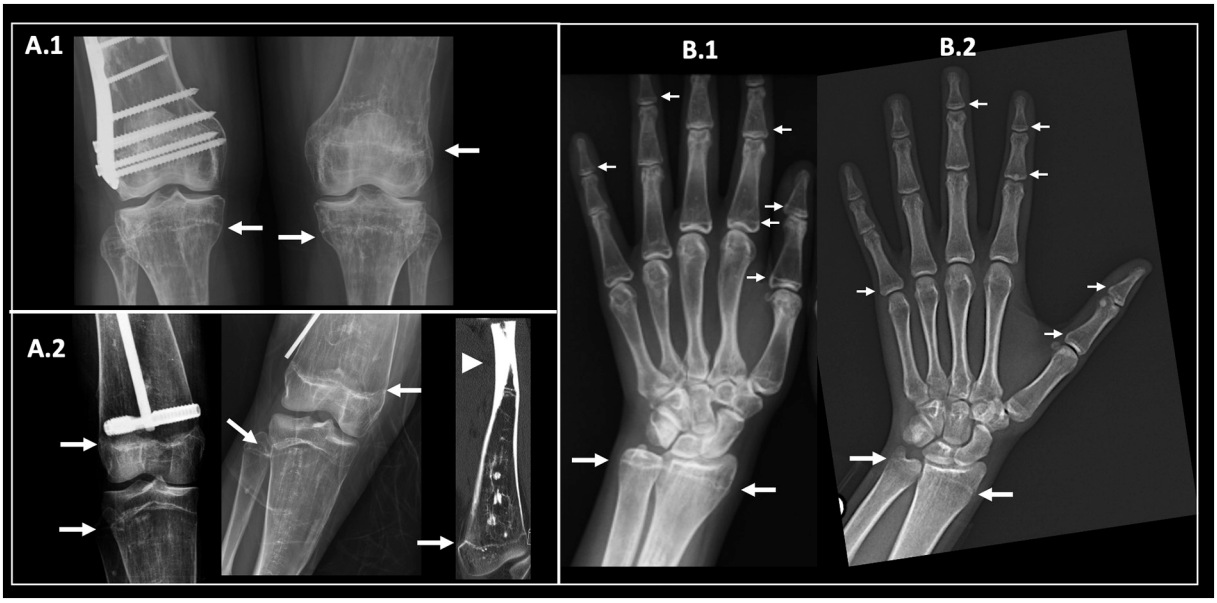

Fig. 2. A sclerotic band (arrows) at the fused growth plate at age of 22 years in a case with *SLC29A3*-associated DSS followed previous metaphyseal sclerosis (A.1, B.1). The sclerotic band on radiographs and computerized tomography is also detectable in *TNFRSF11A*-associated DSS at the age of 20 years, but where the radiographs in early ages were not available (A.2, B.2). Arrowhead indicates focal osteosclerosis at mid-diaphysis of the femur.

osteosclerosis [12,37,38]. Short tubular bones of hand can be normal or mildly under-modeled. Furthermore, demarcated focal sclerosis in the diaphysis of long bones leads to the fracture-prone dense bone within the radiolucent long bone [12,37] (Fig. 2). The short and widened femoral neck and, almost normal vertebral height with dorsal wedging are other radiological features [37,38]. Nonetheless, radiological findings during early childhood and their change with age, the presence of isolated metaphyseal osteosclerosis during infancy or early childhood need to be explored in these cases. A sclerotic band at the metaepiphyseal junction, where the closed growth plate is localized, may be seen in those with *TNFRSF11A*-associated DSS [12,37,38]. This sclerotic band is also identified in adulthood in cases with proven past metaphyseal osteosclerosis [11,37,50] and can be a sign of former metaphyseal and/or epiphyseal sclerosis (Fig. 2). Therefore, it is possible that metaphyseal osteosclerosis is part of radiological features in *TNFRSF11A*-associated DSS.

3.3. TCIRG1-associated DSS

The radiological findings of two siblings with biallelic *TCIRG1* mutations demonstrated diffuse femoral osteosclerosis with Erlenmeyer flask deformity and short femoral neck [13]. However, in these patients the radiological features were more compatible with DSS, not OPT such as metaphyseal and focal osteosclerosis of the humerus and metacarpal bones, mild sclerosis of the axial skeleton with sandwich vertebrate and platyspondyly, and, mild skull base sclerosis.

3.4. CSF1R-associated DSS

The radiological findings of the DSS-Pyle phenotype with biallelic *CSF1R* defects are characterized by osteosclerosis of the axial skeleton with undertubulation of long and short tubular bones demonstrating remarkable Erlenmeyer flask deformity [17,42]. Furthermore, similar to *SLC29A3* mutations [5,6,37], widened radiolucent metaphysis and diaphysis have thin cortices, additionally, a demarcated osteosclerotic bone section exists at relatively narrow mid diaphysis similar to *TNFRSF11A* defects [13,37]. Although longitudinal follow-up of radiographic changes has not been undertaken, it is likely that widened diaphysis is not radiolucent but rather osteosclerotic in early childhood [17]. Additionally, typical metaphyseal osteosclerosis, as seen in *SLC29A3* defects, seems not to be a feature of *CSFR1* defects but rim-like metaphyseal sclerosis is detectable in early childhood (Family A-Patient III-1) and it is possible this gives rise to a remnant sclerotic band when the growth plate fused (Family B- Patient II-1) [17]. Sclerosis of cranial bones especially skull base, mild vertebral end plate sclerosis, and mild platyspondyly, or concavity of the posterior third of vertebral bodies are other distinguishing features [17,42].

Two different reports of biallelic *CSFR1* mutations in 2017 [54] and 2019 [55] with lethality in the early neonatal and infancy period and severe brain malformations demonstrated generalized osteosclerosis in both, and, irregular metaphysis in one [54,55]. Although these two reports did not display typical DSS bone phenotype, it is unknown whether generalized osteosclerosis would evolve to a DSS phenotype with age. Furthermore, one historical DSS case with intracranial calcification and convulsions, reminiscent of *CSFR1* defects, had metaphyseal radiolucency at birth and developed metaphyseal sclerosis and under-modeled long bones, i.e. DSS phenotype, later in life at 13 months of age [9]. Although his initial bone findings were not described as generalized osteosclerosis, the patient was born prematurely at 31 weeks and the bones appear quite dense for a premature baby. Thus, generalized sclerosis with metaphyseal radiolucency/changes could be a sign of future DSS phenotype in *CSF1R* defects. The probable mechanisms are detailed below in the pathogenesis section.

Monoallelic mutation of *CSF1R* is associated with adult-onset rapidly progressive neurodegenerative disorder-hereditary diffuse leukoencephalopathy with spheroids (HDLS) [1]. While no bone changes were reported in large series of HDLS [56], more recently, an HDLS case with heterozygous *CSF1R* mutation (p.Q481*) was reported to have the sclerotic bone disease by Breningstall et al. [43]. This was a 14-year-old male that presented with typical clinical and radiological features of HDLS [43]. The radiographs, kindly provided by Dr. G. N. Breningstall (unpublished), illustrate the typical DSS phenotype with sclerosis of cranial vault, under-modeled long and short tubular bones with flared radiolucent metaphysis and sclerotic diaphysis, dorsal wedging of flattened vertebral bodies with end plate sclerosis and, unevenly sclerotic pelvic bones and flared ribs (Fig. 3). Thus, not only the biallelic mutation but also monoallelic mutation potentially cause sclerotic bone dysplasia i.e. DSS, but not all cases with biallelic mutation lead to bone changes.

3.5. LRRK1-associated DSS

The *LRRK1* mutations have been described as a cause of 'Osteosclerotic metaphyseal dysplasia (OMD)', as the name suggested, metaphyseal sclerosis is the prominent finding [16,48–52]. Ten individuals have been reported with homozygous defects of *LRRK1*. The radiographic features resemble those attributable to historically or genetically proven DSS including *SLC29A3* or *TCIRG1* defects [5,6,13,34,36,37]. Similarly, metaphyseal osteosclerosis is one of the earliest findings, and, after childhood, likely fades and is not detected during adulthood, but a sclerotic band at the closed epiphyseal plate [48,50]. The mild undertubulation of long and short tubular bones is also a feature of *LRRK1*-associated DSS [16,48,51]. Nevertheless, the changes in the axial skeleton might be milder such as no prominent platyspondyly, and mild sclerosis of the cranial base in general [16,48]. However, more recently, significant morbidities related to the thickening of cranial bone/vault, i.e. optic atrophy, conductive hearing loss and osteomyelitis of the jaw have also been detected from early childhood [51,52] in addition to osteonecrosis and multiple fractures of the mandible in adulthood [50]. The end plate sclerosis gives the impression of sandwich vertebrae, and, broad and sclerotic ribs during childhood become broad and corticospongious in adulthood [50].

As a result, radiological findings seen in all four genetic defects are more or less similar, and the differences are most likely related to the severity of the genetic defect and/or the age at which the radiological examination is performed.

3.6. Bone mineral density

Areal bone mineral density measurements (aBMD) with dual-energy X-ray absorptiometry (DXA) might be a useful tool in determining the severity of osteosclerosis in DSS. However, aBMD data for DSS are scarce and reported almost only in individuals with *SLC29A3* defects. Lumbar spine DXA z-scores are over +5 in all reported individuals with biallelic *SLC29A3* mutations [5,6,34,37], but, normal lumbar DXA z-score was detected in one patient with mild osteosclerosis, in early childhood [36]. Progression of lumbar DXA aBMD shows differences from patient to patient, such as; one patient showed increment from +8.1 at 2 years of age to +11.9 at 5 years of age, while progressive decrement from +8 at 20 months of age to +5.1 at age 5.5 years was observed in another [5,34]. Additionally, we observed a waxing and waning course of DXA z-score from age 7 years to 23 years between +10.8 and + 5.6 in a patient with homozygous c.303_320dup variant in *SLC29A3* [37], yet, this variant was also found to be homozygous in a case with normal lumbar DXA z-score (+0.6) [36]. Furthermore, we demonstrated an increment of L_1-L_4 aBMD z-scores from +8.1 at 18 years of age to +10.7 at 21 years of age in a patient with *TNFRSF11A*-associated DSS [37]. However, it must be kept in mind that aBMD measurement with DXA shows variations according to instruments used and body size. The z-scores given for the patients may not be body size corrected values and the z-score can be higher than reported since the patient usually have short stature.

In summary, osteosclerotic wide metaphysis is the earliest recognizable finding for DSS, and the extent and progression of metaphyseal osteosclerosis changes with age, but vanishes up to the adolescent years. However, a phantom sclerotic band at the epiphyseal plate after fusion of epiphysis could be a sign of earlier metaphyseal osteosclerosis. If the patients present at older ages after fading of metaphyseal sclerosis; radiolucency, patchy and/or focal sclerosis of long and/or short bones with varying degrees of undertubulation could be suggestive of DSS. Although the spinal aBMD z-score changes with age, axial skeleton sclerosis is relatively more consistent all through the years with vertebral endplate sclerosis, variable widened sclerotic ribs, and, osteosclerosis of pelvic bones and the cranial base. Platyspondyly has been described as the principal finding of DSS, yet, it is variable and may not

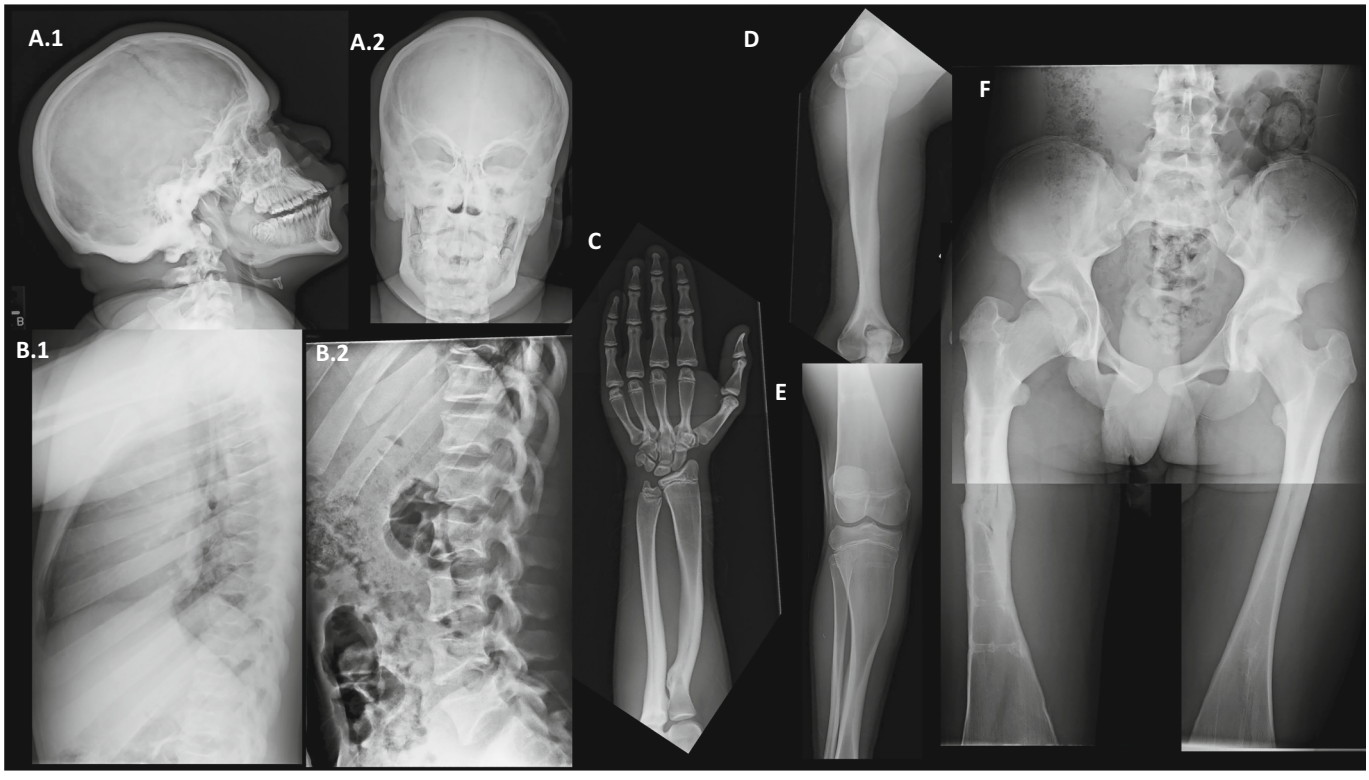

Fig. 3. Radiographs of an osteosclerotic adolescent boy with hereditary diffuse leukoencephalopathy with spheroids (HDLS) reported by G. N. Breningstall et al. shows sclerosis of the cranial vault (A.1) and mandible (A.2), dorsal wedging of flattened vertebral bodies with endplate sclerosis at the thoracic (B.1) and lumbar spine (B.2), and flared osteosclerotic ribs (B.1, B.2), under-modeled long and short tubular bones with flared radiolucent metaphysis, sclerotic diaphysis, and healing fracture of the left femur (C—F) and, unevenly sclerotic pelvic bones (F). The radiographs are published courtesy of Dr. G. N. Breningstall.

be detected in all cases at initial presentation [37]. Moreover, the subjectivity of vertebral height evaluation and segmental vertebral height differences can make the recognition of platyspondyly tricky, especially in mild cases. Therefore, evolving features of radiological findings make the diagnosis of DSS challenging.

4. Biochemical laboratory findings

In the biochemical evaluation of DSS; bone turnover markers (BTMs) vary according to the genetic etiology and/or pathophysiology, and give information about the functional properties of osteoclasts and osteoblasts, and, some changes in calcium metabolism might also be detected.

The BTMs in patients with *SLC29A3* mutations showed low tartrate-resistant acid phosphatase 5b (TRACP-5b) concordant with osteoclast poor OPT [5,34], whereas, RANKL is elevated, probably due to paucity of osteoclasts causing resistance or non-responsiveness [34]. However, other bone resorption and formation markers show inconsistent results, such as: normal to elevated urinary deoxypyridinoline (DPD), low to normal serum alkaline phosphatase (ALP), low bone-specific ALP (BAP) levels, and low to high osteocalcin levels, while C-terminal telopeptide (CTx), and, procollagen type 1 N-terminal propeptide (P1NP) levels are normal in all evaluated cases [5,34,37]. These variable results were obtained from different patients or the same patient at different ages. Although it is impossible to detect exact etiology, the variations in BTMs could be related to the existence of fractures or microfractures, since fractures affect both bone formation and bone resorption. Furthermore, in DSS, bone phenotype changes from increasing osteosclerosis to a fading osteosclerosis phase and it is possible that BMTs reflect the phases of the disease.

Similarly, BTMs from two patients with *TNFRSF11A*-associated DSS show low normal TRACP-5b levels with normal CTx and DPD levels and undetectable serum BB isoenzyme of creatine kinase [37,38], hinting at a mild osteoclast defect. Low to low/normal levels of P1NP and normal ALP levels may be indicative of a mild osteoblast defect [37,38].

Likewise, low ALP levels were also detected in a patient with homozygous CSFR1 mutation, yet, the levels of TRACP-5b, CTx, and type I collagen cross-linked N-telopeptide (NTx) were normal [17]. Furthermore, one historical case with clinical DSS-Pyle diseases phenotype had low BAP and low/normal parathyroid hormone (PTH) and, elevated 1,25(OH)2 vitamin D levels with normal calcium, phosphate calcitonin levels and probably normal TRACP level [9]. These results are not conclusive for etiopathology.

No detailed BMTs were studied in patients with *LRRK1* defects [48–52] but low ALP level was detected in one patient who had also elevated levels of creatine kinase, aspartate aminotransferase, alanine aminotransferase, and lactate dehydrogenase, related to underlying Duchenne Muscular Dystrophy [16]. While high ALP levels were detected in genetically unproven OMD cases [44].

In general, no abnormality for calcium phosphate metabolism has been detected in DSS cases, yet, hypercalcemia was reported in a patient with *SLC29A3* mutation, related to high intake of calcium [5,6]. We also detected severe hypercalcemia in a patient with no detectable mutation, who responded well to bisphosphonate treatment without any further recurrence [37]. Nevertheless, low-normal PTH levels have been detected in several individuals with different DSSs as an indirect finding of hypercalcemia [6,9,37]. Additionally, one patient with biallelic severe *CSF1R* defect, who showed OPT phenotype, was reported to have low serum calcium levels requiring intravenous calcium replacement [55]. Similarly, one patient with homozygous truncating *TNFRSF11A* mutation (p.R7Cfs*172) had hypocalcemia, and, the biochemistry was consistent with osteopetrorickets [41]. Therefore, it can be conceivable in DSS that the more severe osteoclast defects cause hypocalcemia due to the bone resorption defect, while the abnormal function of osteoclasts and osteoblasts may lead to hypercalcemia potentially related to high calcium intake, abnormal bone resorption, and/or bone formation/mineralization defect in DSS (See below).

These findings suggest that the osteoclast defect is a primary problem in DSS and, low formation markers point towards DSS as a low bone turnover disease. Additionally, abnormal regulation of calcium and phosphate metabolism is likely.

5. Histopathology

The earliest histopathological analysis of the DSS cases showed abnormality of growth plate cartilage as less organized columniations [7]. Heavy mineralization of unresorbed cartilage and immature osteoid was detected [7]. The replacement of the calcified cartilage by bone or osteoid was not exhibited [7,10]. Biopsy from compact bone showed no cartilage tissue and osteoclast, additionally, the paucity of osteoblasts with diminution of vascularity was detected [10].

5.1. *SLC29A3-associated DSS*

After revealing genetic etiology, several in vivo and in vitro data from the *SLC29A3* defects shed light on the etiopathogenesis of DSS. Similar to the earlier studies, the disordered growth plate where osteosclerosis is observed on radiographs, together with the absence of osteoclast are the main findings [5]. A more detailed histopathological analysis of physeal zone showed normal proliferation and hypertrophy of chondrocytes, yet, their usual columnar orientation was disrupted. However, an area deep to the growth plate, where normally trabecular bone is present, illustrated modest amounts of centrally localized and almost entirely calcified cartilage remnants. Diminished numbers of hematopoietic cells among the calcified cartilage were detected, instead, primarily mesenchymal cells like osteoblasts and fibroblasts were seen. Osteoclasts were not identified either by morphological examination or by TRAP staining [5]. Overall, the findings of the absence of distinguishable osteoclasts with increased amounts of calcified cartilage and diminished hematopoietic marrow are consistent with “osteoclast-poor” OPT. Furthermore, the peripheral blood monocytes (PBMs) isolated from two patients with biallelic *SLC29A3* defect showed impairment of osteoclastic differentiation and also marked reduction in vitro of the demineralization capacity of the differentiated osteoclasts [6]. Supporting the role of *SLC29A3* in osteoclast biology, Slc29a3 is expressed as a strong punctate pattern in the cytoplasm of multinucleated cells revealed by immunohistochemistry in mouse bones [6].

Histopathological analysis of our patient with *SLC29A3* mutation, using the supracondylar specimen of the femur where the recurrent fracture occurred, showed focal, irregular, lytic, and dysplastic enchondral bone adjacent to mature compact bone [37]. This finding suggests dysplastic repair of the fractured bone, probably related to the resorption and/or remodeling defects. Therefore, delayed healing of fractures may occur [5,37], and recurrent fractures may present at dysplastic bone sites as well [37]. Supporting this hypothesis, no normal bone formation was found by fluorescence imaging after demeclocycline exposure, and diffuse uptake was detected in areas of calcified cartilage near the growth plate [5]. BTMs also support these histopathological findings with low bone formation and low bone resorption markers.

5.2. *TNFRSF11A-associated DSS*

There is no histopathological finding yet for *TNFRSF11A*-associated DSS. However, in *TNFRSF11A*-related OPT; histopathological analysis revealed few or absent osteoclasts, and, few patient-derived PBMs differentiated to osteoclasts upon exposure to M-CSF and RANKL [14,57]. Similarly, PBMs from one individual with *TNFRSF11A*-associated DSS showed an osteoclast differentiation defect with fewer TRAP positive cells than normal [38]. Nevertheless, BMTs (i.e. TRACP-5b and CTX) were near normal in DSS cases, indicating a less severe osteoclast defect in *TNFRSF11A*-associated DSS than OPT [37,38]. Although no histopathological evidence exists yet, bone formation is likely affected in DSS, since patients have low P1NP levels [37,38].

5.3. CSF1R-associated DSS

For *CSF1R*-associated DSS; iliac crest biopsies from a 14 year old boy showed islands of calcified cartilage in areas of woven bone deep into the growth plate, but not in the lamellar bone. Additionally, more intense calcification of these cartilage remnants in comparison to bone was detected by back-scattered electron microscopy [17]. Although no information about osteoclasts could be retrieved from the patients, impaired osteoclastogenesis has been detected in *Csf1r* KO mice, their bone phenotype is described as osteoclast poor-OPT [58,59]. *Csf1r* deficiency in mice and zebrafish mirrors the bone and neurological phenotype of the human DSS-Pyle Disease spectrum [55,58]. Bone remodeling was impaired, and increased trabeculae were detected in the expanded epiphyseal chondrocyte region. Histological sections showed decreased TRAP-stained cells in *Csf1r* KO mice [58]. Based on these findings, *CSF1R*-associated DSS can be described as osteoclast-poor osteosclerotic bone disease. However, osteoclast markers i.e. TRAP-5b, CTx, and NTx, measured in patients with *CSF1R*-associated DSS were normal [17], and there was a milder phenotype compared to *Csf1r* KO mice, most likely explained by hypomorphicity of the human pathogenic variants.

In addition to few osteoclasts, abnormal bone formation and severely distorted bone matrix with a mineralization defect and disorganized collagen fibrils point to a functional defect of osteoblasts [59]. However, osteoblasts do not express Csf1r, and the absence of an osteoblast defect in the early embryonal period before the appearance of osteoclasts, and correction of bone formation defect after transplantation, indicate the primary problem involves the osteoclast affecting osteoblast function in *CSF1R*-associated DSS [59].

Similarly, the defective bone formation is hinted at by the decreased osteoblast markers, i.e. serum osteocalcin, ALP, and P1NP levels in several patients with DSSs, especially with osteoclast-poor genotypes [5,37,38]. As demonstrated in *Csf1r* KO mice, the mineralization defects of the long bones with thin cortex could be from abnormal bone formation/osteoblastogenesis, not defective osteoclastogenesis, but rather the indirect effect on osteoblast function.

The potential effect of the osteoclast on osteoblastogenesis is mediated through osteoclast-osteoblast cross-talk involving RANK/RANKL signaling/vesicular RANK reverse signaling that involves OPG [62]. Therefore, decreased number of osteoclasts and/or RANK deficiency prohibit osteoblast differentiation and function, a likely mechanism for osteoblast dysfunction with the abnormal bone formation in DSS.

5.4. TCIRG1-associated DSS

While defects of the first two genes, i.e. *SLC29A3* and *TNFRSF11A*, as well as *CSF1R,* cause osteoclast-poor DSS, *TCIRG1* was the third gene described in association with DSS, and is known to be a cause of osteoclast-rich OPT [13,61,62]. Histopathological analysis was not performed in the two patients with *TCIRG1*-associated DSS, yet osteoid accumulation and bone marrow fibrosis in addition to the high osteoclast numbers are described in *TCIRG1*-related OPT [61]. However, retained mineralized cartilage and primary spongiosa in *TCIRG1*-related OPT is similar to the histopathology of DSS patients [62]. BTMs and ALP levels were especially variable in *TCIRG1*-related OPT since osteopetrorickets featuring a mineralization defect causing osteoid accumulation results from the added burden of calcium malabsorption due to defective TCIRG1 in gastric parietal cells [61,62]. Therefore, *TCIRG1*-related DSS histopathology seems unique compared to other forms of DSSs. Additionally, mostly normal lamellar bone with well-formed trabecular bone is characteristic of *TCIRG1*-related OPT. In *TCIRG1*-associated DSS, osteosclerosis of the femora, tibiae, and fibulae is relatively uniform, which can be a radiological sign of its histopathological findings [13].

5.5. LRRK1-associated DSS

Another defect causing the osteoclast-rich DSS phenotype is *LRRK1* mutation [16,59]. Histopathological analysis of a 34-year-old patient harboring a homozygous mutation demonstrated increased trabecular bone mass with few eroded surfaces and unresorbed calcified cartilage remnants throughout an iliac bone biopsy sample [50]. However, abnormal osteoclast function, not impaired osteoclastogenesis, is the defect, as shown by several multinucleated flat-shaped osteoclasts with no visible resorption lacunae [50]. PBMs from the patient showed faster differentiation to osteoclasts but the *LRRK1*-deficient osteoclasts themselves demonstrated abnormal resorption activity with a much lower number and area of resorption pits [50]. *Lrrk1* KO mice have a bone phenotype that closely resembles what is found in patients with biallelic *LRRK1* defects [16]. The histology of the growth plate corresponds to the radiological metaphyseal changes of an expanded hypertrophic zone with delayed replacement of cartilage by endochondral ossification [16]. Similar to *LRRK1*-deficient osteoclasts, osteoclast precursors from *Lrrk1* KO mice differentiate normally into mature TRAP-positive multinucleated cells, but these cells failed to form peripheral sealing zones and ruffled borders [63]. However, *Lrrk1*-deficient cells exhibit a severe reduction of resorption pit area, whereas the mutant *LRRK1*-expressing osteoclasts exhibit a milder defect, suggesting a hypomorphic effect of the mutation on LRRK1 function [16]. Consistent with the histopathological findings, BTMs in *Lrrk1* KO mice showed elevated TRAP5b, a marker of osteoclast number, and decreased serum Ctx-1 level, a marker for osteoclast activity. Furthermore, similar to osteoclast-poor DSS, a mild reduction of serum ALP activity was detected in *Lrrk1* KO mice and in one patient with biallelic *LRRK1* mutation [16].

In summary, DSS pathology features unresorbed calcified cartilage islands in-between trabecular bone at the physea metaphyseal zone, which can reflect osteoclast-poor or osteoclast-rich histopathology. The feature differentiate that DSS from OPT seems to be the timing and severity of the osteoclast defect, which is milder in DSS, together with a defect in osteoblastogenesis and bone formation.

6. Pathogenesis

In this section, *SLC29A3, CSF1R,* and *LRRK1* will be discussed, whereas the other two genes (*TCIRG1* and *TNFRSF11A*) are reviewed elsewhere in this special issue.

6.1. SLC29A3 (OMIM *612373) defects

SLC29A3, the first gene associated with DSS, is a member of the *SLC29* gene family which encodes four nucleoside transporters (ENTs; ENT1 to ENT4) [64]. *SLC29A3* is on chromosome 10 (10q22.1), contains six exons, and encodes equilibrative nucleoside transporter 3 (ENT3), a protein of 465 amino acids [65]. ENTs mediate membrane translocation of hydrophilic nucleosides to regulate salvage DNA synthesis and purinergic signaling [64]. ENT3 is the only intracellular nucleoside transporter in the family, is localized in late endosomes, lysosomes, and mitochondria and, is unique in its functions with maximal activity at an acidic pH range of 5.5–6.5 [66,67].

Although biallelic *SLC29A3* mutations have been described as a cause of DSS [6,34–37], a series of disorders with dermatological, musculoskeletal, endocrinological, and hematological manifestations has also been related to *SLC29A3* mutations [68]. These have been clarified as four distinct disorders initially; Faisalabad histiocytosis (FHC), H syndrome, sinus histiocytosis with massive lymphadenopathy (also known as familial Rosai-Dorfman disease), and pigmented hypertrichosis and insulin-dependent diabetes (PHID), but now reclassified as a single entity histiocytosis-lymphadenopathy plus syndrome (HLPS) (OMIM #602782) [1]. The principal pathology for histiocytosis-lymphadenopathy spectrum complications in ENT3 disorders is

impaired macrophage function. *SLC29A3* mutations disrupt nucleoside transport, subcellular localization, protein stability, and pH sensing, with the residual function of ENT3 determining the severity of the disease [65,67,69–71]. Currently, more than 40 mutations have been associated with HPLS and/or DSS, and, among them; 6 mutations are associated with the DSS phenotype [6,34–37]. However, two mutations described in DSS are also found to cause HLPS (p.R386Q and p.T449R) [6,72,73]. p.R386Q variant was first described as homozygous in a Syrian family with HLPS in 2012, in whom no bone phenotype was detected [72]. Then, it was identified as the cause of DSS in a compound heterozygous state with p.S203P variant in a patient of Turkish descent [6], and homozygous in a Cameroonian patient [34]. Homozygous p.T449R mutation caused DSS and HPLS in one family of unknown descent [6] and one Lebanese family respectively [73]. However, HLPS has not been reported in any patient with DSS, or DSS in any case with HLPS. Although a functional assay was not performed for all known mutations, and genotype-phenotype correlation has not been defined, reduction of nucleoside transport activity is mildest with the p.T449R mutation among the 7 studied mutations thus far [65]. Therefore, possibly the functional properties of different mutations affect the disease phenotype and its evolution. All mutations and their related phenotype are given in Fig. 4.

The mouse ENT3 (mENT3) knock-out (KO) model (*Slc29a3*$^{-/-}$) recapitulates the human phenotypes, seemingly normal until 10–12 weeks of age [68,74]. However, after 12 weeks of age, health deteriorates with almost 90 % mortality at 18–20 weeks apparently from unrelated disorders. Necropsy findings identify reduced bone marrow cellularity, massive enlargements of the spleen and occasionally the liver, with severe histiocytosis in numerous organs. Thus, *Slc29a3*$^{-/-}$ mice display several characteristics analogous to human HPLS [74,75].

Slc29a3$^{-/-}$ mice demonstrate a 'hunchback" kyphosis, dental malocclusion, and skeletal deformities consistent with impaired bone and cartilage development, and hypertrichosis at 12 weeks of age; i.e. as adults (human equivalent 42.5 years). MicroCT displayed loss of trabecular bone mineral density in *Slc29a3*$^{-/-}$ mice [75]. Further studies showed abnormal differentiation of mesenchymal stem cells (MSCs) and hematopoietic stem cells (HSCs). MSCs from adult mice were defective in forming mesenchymal lineages, such as osteoblasts, and chondrocytes, adipocytes, and myocytes had reduction in lineage-specific cellular markers [75]. An additional feature was increased osteoclastogenesis from colony-forming unit-macrophage (CFU-M) cells with enhanced differentiation of CFU-M from HSCs, altogether elucidating the skeletal deformities and aberrant bone mineralization in adult *Slc29a3*$^{-/-}$ mice [75]. Contrary to *Slc29a3*$^{-/-}$ mice, osteoclast differentiation is impaired in human PBMs obtained from DSS patients [6]. Inconsistent results associated with human versus mouse osteoclastogenesis from *SLC29A3* defects might be related to testing different cell types (i.e. HSCs in mice, PBMs in patients), and use of adult HSCs from mice whereas human specimens were from children. Despite the different methods and organisms, the different responses from adult versus juvenile cells perhaps explains the age-dependent changes in the bone phenotype of DSS. While the bone phenotype is characterized by osteosclerosis in early childhood in those with *SLC29A3*-associated DSS, the osteosclerosis decreases and osteopenia becomes a more prominent finding by adulthood [37]. These findings from patients with DSS indicate increased osteoclast activity and/or impaired osteoblast function in adulthood, which is consistent with data from MSCs and HSCs studies in *Slc29a3*$^{-/-}$ adult mice. Adult stem cells act crucially to repair and maintain adult tissues including bone tissue [76]. Hence, the bone phenotype in *SLC29A3*-associated DSS at older ages can be related to the adult stem cell defect, and this issue merits exploration.

Further why a DSS or OPT-like bone phenotype is absent in *Slc29a3*$^{-/-}$ mice might reflect the age of the mice, only adult mice were studied for the bone phenotype after it had developed [74,75]. A bone

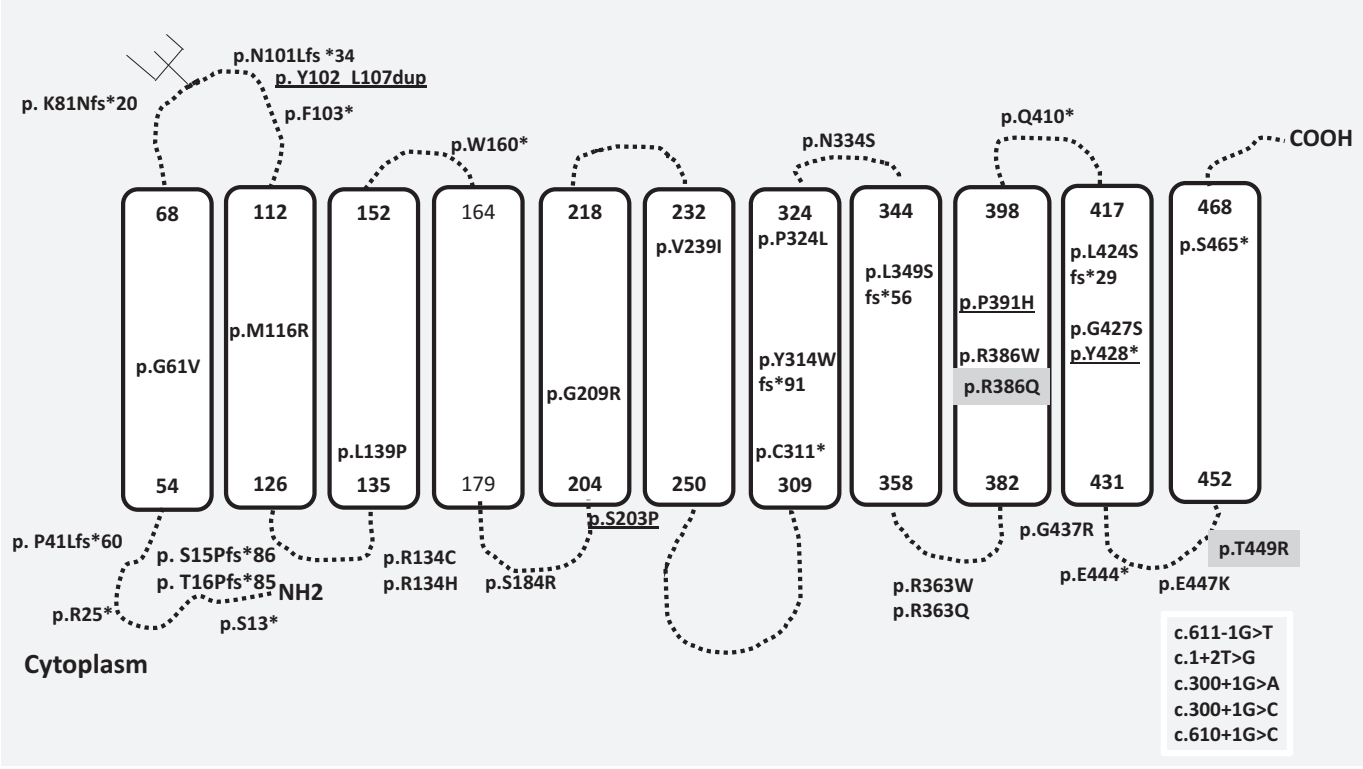

Fig. 4. Schematic diagram of ENT3 (Equilibrative Nucleoside Transporter 3) protein encoded by *SLC29A3* gene and its mutations related to dysosteosclerosis (DSS) and/or histiocytosis-lymphadenopathy plus syndrome (HLPS) are shown. Mutations associated with DSS are underlined and mutations related to both HPLS and DSS are in the gray box. Five splice site mutations are given separately. The data was retrieved from HGMD (Human Gene Mutation Database) Professional 2022.1 and the publicly available version of the databases (June 23rd 2022).

phenotype was not searched for in young mice, or mimics the human DSS before the deformities occurred in adult mice. Therefore, mouse studies must extend to younger mice including the neonatal period. Although the phenotype in *SLC29A3*-associated DSS is well established in humans [5,6,34–37], a better in vivo model is required for understanding pathophysiology. Additionally, perhaps not all the mice *Slc29a3*$^{-/-}$ model develop a DSS phenotype since only a few patients with *SLC29A3* mutation have the DSS phenotype.

6.2. CSF1R (OMIM *164770) defects

The *CSF1R* gene, located on chromosome 5 (5q32), consists of 21 small exons and encodes a tyrosine kinase growth factor receptor for colony-stimulating factor-1, the macrophage- and monocyte-specific growth factor [77,78]. The CSF1R is expressed in primitive multipotent hematopoietic cells, mononuclear phagocyte progenitor cells, tissue macrophages, osteoclasts, and microglia [79]. Phosphorylation of CSF1R through ligand binding activates multiple downstream kinase pathways, including PI3K, ERK1/2, and JNK. Furthermore, the decreased phosphorylation in JNK has been detected for all the variants thus far identified in the affected individuals, demonstrating functional deficiency [17]. JNK activation is critical for macrophage development and prevention of microglial cell apoptosis [80–81].

Bi-allelic mutations of *CSF1R* in humans are associated with epilepsy, structural brain anomalies, and white matter abnormalities including periventricular calcifications and leukodystrophy, yet are variably associated with sclerotic bone dysplasia, and called “DSS-Pyle disease” or “brain abnormalities, neurodegeneration, and dysosteosclerosis” (BANDDOS: OMIM # 618476) [1,17,42,43,56]. Heterozygous inactivating mutations of *CSF1R* cause a dominantly inherited adult-onset progressive dementia, currently defined as hereditary diffuse leukoencephalopathy with spheroids 1 (HDLS1 OMIM # 221820) [1,56,82].

Targeted ablation of *Csf1r* in mice causes a similar skeletal and neural phenotype with severe decreases in osteoclasts in bone and microglia in the brain [58,59,83]. Specifically, bi-allelic inactivation of *Csf1r* causes severe osteosclerosis and developmental brain anomalies, leading to early death [59]. However, patients with biallelic *CSF1R* mutations have milder phenotypes than *Csf1r* KO mice, suggesting hypomorphic rather than amorphic mutation of at least one allele in affected individuals. However, two siblings with the perinatal lethal phenotype, reported by Monies et al., who possibly carry homozygous *CSF1R* c.1620 T > A (p.Tyr540*), had severe CNS structural anomalies leading to perinatal death [54]. Another patient with a biallelic splice site variant in *CSF1R* (c.17541G > C) had a severe neurological phenotype and survived longer with prolonged intensive care [55]. Thus, perhaps *CSF1R* gene dosage determines survival as patients with biallelic amorphic mutations have more severe anatomical neurological changes leading to early death.

Additionally, patients with early mortality had generalized osteosclerosis interpreted as OPT [54]. The patient who survived infancy had hypocalcemia requiring intravenous calcium and his bone phenotype was described as OPT with irregular metaphyses [55]. Although detailed biochemical features are not known for this patient, hypocalcemia together with metaphyseal changes may indicate osteopetrorickets. The individuals with biallelic *CSF1R* mutations have skeletal phenotypes that change from severe osteosclerosis to milder or no bone phenotype, perhaps depending on the severity of functional loss of the mutations [17,42,43,54,55,84]. While the patient carrying two amorphic, or a combination of hypomorphic and amorphic, alleles demonstrates a skeletal phenotype ranging from OPT to DSS [17,54,55], no or minimal skeletal changes can be found in patients with biallelic hypomorphic mutations [55,84,85]. Variants detected in HDLS are amorphic heterozygous mutations, and classically bone involvement is not detected as a clinical feature of HDLS [56,85]. Moreover, monoallelic deletion of *Csf1r* in mice also shows no bone phenotype, while recapitulating the neurological findings of HDLS [58,59,86]. However, osteosclerotic bone changes mimicking DSS were described by Breningstall et al. (Fig. 3) in an adolescent boy with rapid neurological deterioration. [43]. His mutation (p.Q481*) causes a severe signaling defect with complete loss of function (amorphic mutation) and, was found compound heterozygous in a patient with DSS-Pyle disease [17]. Heterozygous carriers of the mutation in this family displayed no neurological signs, but mild osteosclerosis with increased cortical thickness of long bones. However, the 76-year-old grandfather with the mutation had short-term memory loss that started at age 70 years and one parietal parenchymal calcification on cranial CT [17]. Further definition of bone changes is likely since not all HDLS had been studied for bone phenotyping.

It is hypothesized that HDLS and DSS-Pyle mutations are in different protein domains of CSF1R, HDLS related mutations are mainly located in the intracellular tyrosine kinase domain while DSS-Pyle-related mutations are located in all three domains [56,85]. However, only a few mutations have been detected in the extracellular immunoglobulin-like domain (including p.Q481*) and the transmembrane domain [56,85]. Additionally, several HDLS-related heterozygous nonsense or frameshift mutations (including p.Q481*) undergo nonsense-mediated mRNA decay (NMD) [87]. Thus, the haploinsufficiency of *CSF1R,* or 50 % loss of normal mRNA and protein, could cause the HDLS phenotype [56]. Marked phenotype variation with the same *CSF1R* genotype is not unexpected since the neurological phenotype shows marked variation even within the same family with heterozygous *CSF1R* mutation [56,85]. How haploinsufficiency with 50 % loss of function leads to HDLS at a young age and a bone phenotype, yet no neurological abnormality in others, needs explanation. The reason for phenotypic variation or incomplete penetrance remains unknown, yet, the genetic background could be an explanation since the mono-allelic *Csf1r*-deficient mice show the HDLS phenotype whereas mono-allelic *Csf1r*-deficient rats do not [86,88]. Additional mechanisms could be a dominant negative effect of the abnormal transcript from a mutated allele disrupting stability and/or translation of the wild-type allele and causing more than 50 % loss of function [56], additional unrecognized variants in *CSF1R*, or other effector genes.

Csf1r KO mice have short long bones with metaphyseal osteosclerosis, and mandibular osteosclerosis leading to failure of tooth eruption [58]. Interestingly, similar to the patients with DSS [11,37], *Csf1r* KO mice illustrate bone changes with age as an expansion of metaphyseal osteosclerosis up to the mid-diaphysis of the femur [58]. The metaphyseal osteosclerosis of the long bones is caused by more bony trabeculae and impaired bone remodeling from failure of osteoclast development related to the impaired CSF1R signaling [58]. Targeted ablation of *Csf1r* in FVB/NJ background in comparison with outbred background causes a severe phenotype with death within the first month of life [59]. These mice have exhibited limb deformities caused by spontaneous fractures of long bones and abnormal bone mineralization secondary to the osteoblast defect. The abnormal osteoblast function might be developmental and from functional failure of the osteoclasts [60]. Remarkable findings in the *Csf1r*$^{-/-}$ mice are decreased cortical thickness and marked disorganization of the cortical structure together with a substantial delay in the cartilage mineralization, especially in secondary ossification centers of the long bones and vertebrae [59]. Mineralization defects and spontaneous fractures are consistent with the evolving disease pattern and bone phenotype at later ages [11,37,38,50]. Additionally, a broadened epiphyseal plate from expansion of both proliferative and hypertrophic chondrocytes is consistent with the enlarged radiolucency of the growth plate in *Csf1r*$^{-/-}$ mice, in line with human osteopetrorickets [55,59]. However, biochemical features are not known in the mice model, and whether a calcium-mineral abnormality causes a mineralization defect in *Csf1r*$^{-/-}$ mice needs to be clarification.

In summary, *CSF1R* spectrum disorders show quite variable osteosclerotic phenotypes related to defects in osteoclast development and probably functional osteoblast defects. Although *CSF1R* gene dosage

conditions the phenotype, heterozygous gene variants may cause bone changes.

6.3. LRRK1 (OMIM *610986) defects

The *LRRK1* gene, located on chromosome 15 (15q26.3), consists of 34 exons and encodes a protein of 2015 amino acids which contains 6 N-terminal ankyrin repeats, followed by 14 leucine-rich repeats, a RAS-like GTPase domain (ROC domain), a C-terminal to ROC domain, a serine/threonine kinase domain, and 7 C-terminal WD40 repeats [89].

Lrrk1was initially considered a mammalian growth regulatory factor, and its overexpression induced human HEK293 cell proliferation [90]. However, further studies showed loss of *Lrrk1* led to severe OPT in mice [91]. Later, homozygous *LRRK1* mutation was identified as a cause of sclerotic bone disease defined as OMD in a 14-month-old boy presenting with failure to thrive [16]. Currently, 10 individuals from 6 families with *LRRK1*-associated DSS (or OMD) have been described [16,48–52]. Furthermore, the body length of *Lrrk1* KO mice was slightly short. Patients with *LRRK1* mutations and *Lrrk1* KO mice showed comparable phenotypes [16,91]. Similar to such patients with *LRRK1* defects, *Lrrk1* KO mice had wide metaphysis and metaphyseal and epiphyseal osteosclerosis of poorly modeled long bones. Their short tubular bones showed slightly osteopenic diaphyses, and together with flattening and endplate sclerosis of vertebrae and marginal sclerosis of pelvic bones completely recapitulated the human DSS phenotype [16].

Micro-CT of *Lrrk1* KO mice revealed markedly increased trabecular bone volume due to elevated trabecular number and thickness with reduced trabecular separation. Primary spongiosa extended to the diaphysis, and was characterized by increased mature osteoclasts, cartilage, and trabecular bone, while the secondary spongiosa was incomplete and short [91]. In contrast to the markedly elevated trabecular bone volume in long bones and vertebrae, a slight increase in cortical bone thickness and modest involvement of calvarial bones were detected [91]. These findings may indicate differential regulation of osteoclast function in membranous and endochondral bone. Similarly, thickening of calvarial bone has been reported in 30 % of patients harboring *LRKK1* mutation, and leading to optic atrophy and recurrent osteomyelitis of the jaw and loss of teeth [48,50–52]. Additionally, increased numbers of abnormal osteoclasts together with extended primary spongiosa with retention of cartilage cores indicated impairment of the resorptive capacity of osteoclasts [91]. *Lrrk1* deficient osteoclasts showed reduced resorption pits, which were also smaller and shallower as measured by nano-CT. Thus, *Lrrk1* does not affect osteoclast differentiation, but is essential for osteoclast function. Bone resorption is significantly impaired in Lrrk1 deficiency and demonstrated in patients with *LRKK1* mutation [50]. However, the resorption pit area is not severely reduced in *LRKK1* deficient osteoclasts as *Lrrk1* KO osteoclasts, suggest hypoomorphic effects of mutation on LRRK1 function.

Osteoclasts lacking *LRRK1* failed cytoskeletal rearrangement in response to RANKL, including formation of peripheral sealing zones and ruffled borders, which are related to the abnormal intracellular distribution of F-actin [16,50,91]. LRRK1 functions in serine 5 phosphorylation of L-plastin, a member of the cytoskeleton, that stabilizes actin-based osteoclast sealing rings and podosomes, critical for osteoclast adhesion and the early process of bone resorption [92]. Furthermore, targeted deletion of the *L-plastin* gene in mice causes an OPT phenotype. However, trabecular bone mass deposition is much less in *L-plastin* KO mice compared to *Lrrk1* KO mice [91,92]. Therefore, the phosphorylation defect of L-plastin alone seems insufficient to explain the entire phenotype of Lrrk1 deficiency. The integrin αvβ3, c-Src, and Rac/ cdc42 small GTPase proteins are essential regulators of the osteoclast cytoskeleton and function [93–95]. Deletion of any of these signaling molecules causes an OPT phenotype by impairing the capability of osteoclasts to remodel the cytoskeleton and resorb bone. Similar to L-plastin, mice with disrupted integrin, Src or RAC/Cdc42 proteins show a less severe bone phenotype than *Lrrk1* KO mice [92]. Overall, these findings highlight phosphorylation of multiple substrates by Lrrk1 in downstream Lrrk1 signaling pathways and, L-plastin seems just one Lrrk1 target.

Additionally, the bone formation rate is also reduced in *Lrrk1* KO mice, yet osteocyte density in femur cortical bone and the anabolic effects of PTH are normal [91].

In conclusion, LRRK1 plays a key role in osteoclast cytoskeleton remodeling and formation of a functional resorption pit. This is probably by initiating a cascade of phosphorylation involving several factors. Apparently, bone formation is not severely compromised in *Lrrk1* KO mice, probably related to intact osteoclast formation which maintains RANK-RANKL cross talk and preserves osteoblast function.

7. Summary and future perspectives

DSS is a group of heritable osteosclerotic diseases with unique radiological features. Recognizing their radiographic hallmarks is key to suspecting and diagnosing DSS. Mutations in *SLC29A3*, *TNFRSF11A*, *TCIRG1*, *LRRK1*, and *CSF1R* are now associated with DSS. The bone phenotype in *SLC29A3, LRRK1*, and *CSF1R* DSS is relatively consistent and straightforward features of DSS, bone disease occurs together with variable gene-specific extra-skeletal features. However, defining DSS from mutation of other genes known to cause OPT, i.e. *TNFRSF11A* and *TCIRG1*, can be challenging, since differentiating DSS from OPT is complicated as evolution of radiological features and other clinical findings specific to OPT should be taken into account. Genetic and phenotypic heterogeneity of DSS must be evaluated as the etiology, complications, pathogenesis, and prognosis differ. Nevertheless, not all *TNFRSF11A*- associated DSS has a complete DSS phenotype and could be considered an OPT [39–41], while, other cases reported as *TNFRSF11A*-associated OPT have a DSS phenotype [96]. Indeed, a patient has been reported with *TNFSF11 (RANKL)*-associated OPT and radiological and clinical features of DSS [97]. Therefore, further genetic heterogeneity for DSS seems likely, and related to other OPT genes, including an X-linked recessive DSS [10] and our patient with an unknown genetic defect [37]. Furthermore, the absence of a bone phenotype in some cases with *SLC29A3* and *CSF1R* mutations must be clarified. In clinical practice, establishing the diagnostic criteria and genetic basis for DSS will help understand the complications, prognosis, and treatment.

Furthermore, HSCT is not considered as a treatment option for DSS, however, its complications such as cranial nerve palsies, osteonecrosis of the jaw, and fractures may severely affect quality of life. It should be kept in mind that osteoblast failure is secondary to an osteoclast defect in DSS, and, resolution of bone abnormalities might be possible with HSCT. Therefore, treatment options should be individualized recognizing the benefit hazard ratio in selected patients with severe complications related to the DSS.

CRediT authorship contribution statement

Serap Turan: Conceptualization, Methodology, Data curation, Writing – original draft, Writing – review & editing.

Declaration of competing interest

None.

Data availability

No data was used for the research described in the article.

Acknowledgment

I thank Dr. Galen N. Breningstall, Gillette Children's Specialty Healthcare, St. Paul, Minnesota for the radiographs shown in Fig. 3.

References

[1] Online Mendelian inheritance in man (OMIM), McKusick-Nathans Institute of Genetic Medicine, Johns Hopkins University (Baltimore, MD) and National Center for Biotechnology Information, National Library of Medicine, Bethesda, MD, 14 April 2021. https://www.omim.org.
[2] R.W. Ellis, Osteopetrosis: (Section for the study of disease in Children), Proc. R. Soc. Med. 27 (12) (1934 Oct) 1563–1571.
[3] J. Spranger, C. Albrecht, H.J. Rohwedder, H.R. Wiedemann, Die Dysosteosklerose–eine Sonder form der generalisierten Osteoskerose [Dysosteosclerosis–a special form of generalized osteosclerosis], Fortschr. Geb. Rontgenstr. Nuklearmed. 109 (4) (1968 Oct) 504–512. German.
[4] G.R. Mortier, D.H. Cohn, V. Cormier-Daire, C. Hall, D. Krakow, S. Mundlos, G. Nishimura, S. Robertson, L. Sangiorgi, R. Savarirayan, D. Sillence, A. Superti-Furga, S. Unger, M.L. Warman, Nosology and classification of genetic skeletal disorders: 2019 revision, Am. J. Med. Genet. A 179 (12) (2019 Dec) 2393–2419.
[5] M.P. Whyte, D. Wenkert, W.H. McAlister, D.V. Novack, A.R. Nenninger, X. Zhang, et al., Dysosteosclerosis presents as an "osteoclast-poor" form of osteopetrosis: comprehensive investigation of a 3-year-old girl and literature review, J. Bone Miner. Res. 25 (11) (2010 Nov) 2527–2539.
[6] P.M. Campeau, J.T. Lu, G. Sule, M.M. Jiang, Y. Bae, S. Madan, et al., Whole-exome sequencing identifies mutations in the nucleoside transporter gene SLC29A3 in dysosteosclerosis, a form of osteopetrosis, Hum. Mol. Genet. 21 (22) (2012 Nov 15) 4904–4909.
[7] C.S. Houston, J.W. Gerrard, E.J. Ives, Dysosteosclerosis, AJR Am. J. Roentgenol. 130 (5) (1978 May) 988–991.
[8] D. Chitayat, K. Silver, E.M. Azouz, Skeletal dysplasia, intracerebral calcifications, optic atrophy, hearing impairment, and mental retardation: nosology of dysosteosclerosis, Am. J. Med. Genet. 43 (3) (1992 Jun 1) 517–523.
[9] K. Kobayashi, Y. Goto, H. Kise, H. Kanai, K. Kodera, G. Nishimura, et al., A case report of dysosteosclerosis observed from the prenatal period, Clin. Pediatr. Endocrinol. 19 (3) (2010 Jul) 57–62.
[10] I. Pascual-Castroviejo, C. Casas-Fernandez, V. Lopez-Martin, A. Martinez-Bermejo, X-linked dysosteosclerosis. Four familial cases, Eur. J. Pediatr. 126 (3) (1977 Oct 12) 127–138.
[11] E.G. Lemire, S. Wiebe, Clinical and radiologic findings in an adult male with dysosteosclerosis, Am. J. Med. Genet. A 146A (4) (2008 Feb 15) 474–478.
[12] L. Guo, N.H. Elcioglu, O.K. Karalar, M.O. Topkar, Z. Wang, Y. Sakamoto, et al., Dysosteosclerosis is also caused by TNFRSF11A mutation, J. Hum. Genet. 63 (6) (2018 Jun) 769–774.
[13] A. Howaldt, S. Nampoothiri, L.M. Quell, A. Ozden, B. Fischer-Zirnsak, C. de Collet, Sclerosing bone dysplasias with hallmarks of dysosteosclerosis in four patients carrying mutations in SLC29A3 and TCIRG1, Bone 120 (2018 Dec 8) 495–503.
[14] M.M. Guerrini, C. Sobacchi, B. Cassani, M. Abinun, S.S. Kilic, A. Pangrazio, et al., Human osteoclast-poor osteopetrosis with hypogammaglobulinemia due to TNFRSF11A (RANK) mutations, Am. J. Hum. Genet. 83 (1) (2008 Jul) 64–76.
[15] A. Frattini, P.J. Orchard, C. Sobacchi, S. Giliani, M. Abinun, J.P. Mattsson, et al., Defects in TCIRG1 subunit of the vacuolar proton pump are responsible for a subset of human autosomal recessive osteopetrosis, Nat. Genet. 25 (3) (2000 Jul) 343–346.
[16] A. Iida, W. Xing, M.K. Docx, T. Nakashima, Z. Wang, M. Kimizuka, et al., Identification of biallelic LRRK1 mutations in osteosclerotic metaphyseal dysplasia and evidence for locus heterogeneity, J. Med. Genet. 53 (8) (2016 Aug) 568–574.
[17] L. Guo, D.R. Bertola, A. Takanohashi, A. Saito, Y. Segawa, T. Yokota, et al., Bi-allelic CSF1R mutations cause skeletal dysplasia of dysosteosclerosis-pyle disease Spectrum and degenerative encephalopathy with brain malformation, Am. J. Hum. Genet. 104 (5) (2019 May 2) 925–935.
[18] O. Oncag, F.F. Ozkinay, C. Eronat, Dysosteosclerosis: a case with unique dental findings and SEM evaluation of a hypoplastic tooth, J. Clin. Pediatr. Dent. 23 (4) (1999) 347–352. Summer.
[19] R.N. Sener, O. Yalman, N. Cetingul, S. Tutuncuoglu, K. Kavakli, E.E. Ustun, Dysosteosclerosis: clinico radiologic findings including brain MRI, Comput. Med. Imaging Graph. 21 (1997) 355–357.
[20] J. Leisti, I. Kaitila, R.S. Lachman, M.J. Asch, D.L. Rimoin, Dysosteosclerosis, Birth Defects Orig. Artic. Ser. 11 (1975) 349–351.
[21] J.P. Fryns, L. Vinken, S. Claessens, J. Marien, J. Geutjens, H. Van den Berghe, Dysosteosclerosis in a mentally retarded boy, Acta Paediatr. Belg. 33 (1980) 53–56.
[22] I. Pascual-Castroviejo, A. Rodríguez Balo, J. Ramos Linaza, A. Martínez de Azagra Garde, Rinolicuorrea en un caso de disosteoesclerosis con estenosis del acueducto de Silvio [Rhinoliquorrhea in a case of dysosteosclerosis with sclerosis of the aqueduct of Sylvius], An. Esp. Pediatr. 30 (5) (1989 May) 419–421. Spanish. PMID: 2667417.
[23] L. Stehr, Pathogenese und klinik den osteosklerosen, Arch. Orthop. Unfallchir. 41 (1941) 156–182.
[24] C. Roy, P. Maroteaux, L. Kremp, V. Courtecuisse, D. Alagille, Un nouveau syndrome osseux avec anomalies cutanees et troubles neurologiques [A new bone syndrome with skin anomalies and neurologic disorders], Arch. Fr. Pediatr. 25 (8) (1968 Oct) 893–905. French.
[25] S.A. Temtamy, H.S. Badramy, M. Sami Abdel Meguid, H.M. Safwat, M. Regai El-Meligy, Metaphyseal dysplasia, anetoderma and optic atrophy: an autosomal recessive syndrome, Birth Defects Orig. Artic. Ser. X (12) (1974) 61–71.
[26] W. Kojmane, S. Chaouki, S. Abourazzak, M. Hida, G. Fikri, M. Boubou, et al., Osteomyelitis of the mandible and dysosteosclerosis, Arch. Pediatr. 22 (11) (2015 Nov) 1154–1156.
[27] N.H. Elçioglu, A. Vellodi, C.M. Hall, Dysosteosclerosis: a report of three new cases and evolution of the radiological findings, J. Med. Genet. 39 (8) (2002 Aug) 603–607.
[28] E. John, K. Kozlowski, J. Masel, S. Muralinath, G. Vijayalakshmi, Dysosteosclerosis, Australas. Radiol. 40 (3) (1996 Aug) 345–347.
[29] A. Al Kaissi, G. Kalchhauser, F. Grill, K. Klaushofer, Arthrogryposis multiplex congenital in a child manifesting phenotypic features resembling dysosteosclerosis/osteosclerosis malformation complex; 3DCT scan analysis of the skull base, Cases J. 1 (1) (2008 Jul 23) 56.
[30] A. Maheshwari, K.M. Rao, N. Kohli, Case report: dysosteosclerosis: a unique entity, Clin. Radiol. 51 (1996) 224–228.
[31] C.E. Field, Albers-Schönberg disease. An atypical case, Proc. R. Soc. Med. 32 (4) (1939 Feb) 320–324.
[32] W. Utz, Manifestation der dysosteosklerose im kieferbereich. [Manifestation of dysosteosclerosis in the region of the jaw], Dtsch. Zahnarztl. Z. 25 (1970) 48–50.
[33] G.V. Packota, J. Shiffman, J.M. Hall, Osteomyelitis of the mandible in a patient with dysosteosclerosis. Report of a case, Oral Surg. Oral Med. Oral Pathol. 71 (2) (1991 Feb) 144–147.
[34] C. Seiltgens, F. Rauch, G. Bardai, SLC29A3 pathogenic variant as a causal for dysosteosclerosis, a poor osteoclast form of osteopetrosis, J. Endoc. Soc. 4 (Suppl. 1) (2020) A917.
[35] S. Turan, S. Mumm, G.S. Gottesman, S. Abali, Baş, Z. Atay, W.H. McAlister, M. P. Whyte, Dysosteosclerosis from a unique mutation in SLC29A3, Bone Abstr. 4 (2015) 97.
[36] D. Uludağ Alkaya, E. Akpınar, K. Bilguvar, B. Tüysüz, Resolution of sclerotic lesions of dysosteosclerosis due to biallelic SLC29A3 variant in a turkish girl, Am. J. Med. Genet. A 185 (7) (2021 Jul) 2271–2277.
[37] S. Turan, S. Mumm, C. Alavanda, S.B. Kaygusuz, B. Gurpinar Tosun, A. Arman, M. Huskey, T. Guran, S. Duan, A. Bereket, M.P. Whyte, Dysosteosclerosis: clinical and radiological evolution reflecting genetic heterogeneity, JBMR Plus 6 (8) (2022 Jul), e10663.
[38] J.Y. Xue, Z. Wang, S. Shinagawa, H. Ohashi, N. Otomo, N.H. Elcioglu, et al., TNFRSF11A-associated dysosteosclerosis: a report of the second case and characterization of the phenotypic spectrum, J. Bone Miner. Res. 34 (10) (2019 Oct) 1873–1879.
[39] J.Y. Xue, Z. Wang, S.F. Smithson, C.P. Burren, N. Matsumoto, G. Nishimura, et al., The third case of TNFRSF11A-associated dysosteosclerosis with a mutation producing elongating proteins, J. Hum. Genet. 66 (4) (2021 Apr) 371–377.
[40] J.Y. Xue, P.O. Simsek-Kiper, G.E. Utine, L. Yan, Z. Wang, E.Z. Taskiran, et al., Expanding the phenotypic spectrum of TNFRSF11A-associated dysosteosclerosis: a case with intracranial extramedullary hematopoiesis, J. Hum. Genet. 6 (2021 Jan).
[41] T Kırkgöz B Özkan F Hazan S Acar Özkaya B NalbantogluÖ MA Kulalı S Gürsoy S Ikegawa L. Guo A null mutation TNFRSF11A causes dysosteosclerosis, not osteopetrosis Front. Genet. (in press).
[42] E. Kındış, P.Ö. Simsek-Kiper, C. Koşukcu, E.Z. Taşkıran, R. Göçmen, E. Utine, G. Haliloğlu, K. Boduroğlu, M. Alikaşifoğlu, Further expanding the mutational spectrum of brain abnormalities, neurodegeneration, and dysosteosclerosis: a rare disorder with neurologic regression and skeletal features, Am. J. Med. Genet. A 185 (6) (2021 Jun) 1888–1896.
[43] G.N. Breningstall, M. Asis, Bone disease associated with hereditary diffuse leukoencephalopathy with spheroids, Pediatr. Neurol. 112 (2020 Nov) 44–46.
[44] G. Nishimura, K. Kozlowski, Osteosclerotic metaphyseal dysplasia, Pediatr. Radiol. 23 (6) (1993) 450–452.
[45] E.A. Mennel, S.D. John, Osteosclerotic metaphyseal dysplasia: a skeletal dysplasia that may mimic lead poisoning in a child with hypotonia and seizures, Pediatr. Radiol. 33 (1) (2003 Jan) 11–14.
[46] C.S. Kasapkara, A. Küçükçongar, O. Boyunağa, T. Bedir, F. Oncü, A. Hasanoğlu, L. Tümer, An extremely rare case: osteosclerotic metaphyseal dysplasia, Genet. Couns. 24 (1) (2013) 69–74.
[47] H. Zheng, J. Cai, L. Wang, X. He, Osteosclerotic metaphyseal dysplasia with extensive interstitial pulmonary lesions: a case report and literature review, Skelet. Radiol. 44 (10) (2015 Oct) 1529–1533.
[48] L. Guo, K.M. Girisha, A. Iida, M. Hebbar, A. Shukla, H. Shah, et al., Identification of a novel LRRK1 mutation in a family with osteosclerotic metaphyseal dysplasia, J. Hum. Genet. 62 (3) (2017 Mar) 437–441.
[49] M. Miryounesi, A. Nikfar, M. Changi-Ashtiani, M. Shahrooei, H. Dinmohammadi, T. Shahani, et al., A novel homozygous LRRK1 stop gain mutation in a patient suspected with osteosclerotic metaphyseal dysplasia, Ann. Hum. Genet. 84 (1) (2020 Jan) 102–106.
[50] A. Howaldt, A.F. Hennig, T. Rolvien, U. Rössler, N. Stelzer, A. Knaus, et al., Adult osteosclerotic metaphyseal dysplasia with progressive osteonecrosis of the jaws and abnormal bone resorption pattern due to a LRRK1 splice site mutation, J. Bone Miner. Res. 35 (7) (2020 Jul) 1322–1332.
[51] O. Chorin, G. Chowers, R. Agbariah, S. Karklinsky, O. Barel, I. Bar-Joseph, H. Reznik-Wolf, J. Shamash, B. Pode-Shakked, J.M. Jacobson, R. Huna-Baron, Y. Redler, I. Tirosh, A. Vivante, A. Raas-Rothschild, Broadening the phenotype of LRRK1 mutations - features of malignant osteopetrosis and optic nerve atrophy with intrafamilial variable expressivity, Eur. J. Med. Genet. 65 (1) (2022 Jan), 104383.

[52] S. Chundoo, D.M. McGoldrick, R. Williams, K. McMillan, Osteosclerotic metaphyseal dysplasia, dysosteosclerosis or osteomyelitis? Paediatric case presentation with associated mandibular swelling and a review of the literature, BMJ Case Rep. 15 (5) (2022 May 12), e246789.
[53] G. Sule, P.M. Campeau, V.W. Zhang, S.C. Nagamani, B.C. Dawson, M. Grover, et al., Next-generation sequencing for disorders of low and high bone mineral density, Osteoporos. Int. 24 (8) (2013 Aug) 2253–2259.
[54] D. Monies, S. Maddirevula, W. Kurdi, M.H. Alanazy, H. Alkhalidi, M. Al-Owain, R. A. Sulaiman, E. Faqeih, E. Goljan, N. Ibrahim, F. Abdulwahab, M. Hashem, M. Abouelhoda, R. Shaheen, S.T. Arold, F.S. Alkuraya, Autozygosity reveals recessive mutations and novel mechanisms in dominant genes: implications in variant interpretation, Genet Med. 19 (10) (2017 Oct) 1144–1150.
[55] N. Oosterhof, I.J. Chang, E.G. Karimiani, L.E. Kuil, D.M. Jensen, R. Daza, E. Young, L. Astle, H.C. van der Linde, G.M. Shivaram, J. Demmers, C.S. Latimer, C.D. Keene, E. Loter, R. Maroofian, T.J. van Ham, R.F. Hevner, J.T. Bennett, Homozygous mutations in CSF1R cause a pediatric-onset leukoencephalopathy and can result in congenital absence of microglia, Am. J. Hum. Genet. 104 (5) (2019 May 2) 936–947.
[56] L. Guo, S. Ikegawa, From HDLS to BANDDOS: fast-expanding phenotypic spectrum of disorders caused by mutations in CSF1R, J. Hum. Genet. 66 (12) (2021 Dec) 1139–1144.
[57] A. Pangrazio, B. Cassani, M.M. Guerrini, J.C. Crockett, V. Marrella, L. Zammataro, D. Strina, A. Schulz, C. Schlack, U. Kornak, D.J. Mellis, A. Duthie, M.H. Helfrich, A. Durandy, D. Moshous, A. Vellodi, R. Chiesa, P. Veys, N. Lo Iacono, P. Vezzoni, A. Fischer, A. Villa, C. Sobacchi, RANK-dependent autosomal recessive osteopetrosis: characterization of five new cases with novel mutations, J. Bone Miner. Res. 27 (2) (2012 Feb) 342–351.
[58] X.M. Dai, G.R. Ryan, A.J. Hapel, M.G. Dominguez, R.G. Russell, S. Kapp, V. Sylvestre, E.R. Stanley, Targeted disruption of the mouse colony-stimulating factor 1 receptor gene results in osteopetrosis, mononuclear phagocyte deficiency, increased primitive progenitor cell frequencies, and reproductive defects, Blood 99 (1) (2002 Jan 1) 111–120.
[59] X.M. Dai, X.H. Zong, M.P. Akhter, E.R. Stanley, Osteoclast deficiency results in disorganized matrix, reduced mineralization, and abnormal osteoblast behavior in developing bone, J. Bone Miner. Res. 19 (9) (2004 Sep) 1441–1451.
[60] Y. Ikebuchi, S. Aoki, M. Honma, et al., Coupling of bone resorption and formation by RANKL reverse signalling, Nature 561 (2018) 195–200.
[61] F. Barvencik, I. Kurth, T. Koehne, T. Stauber, J. Zustin, K. Tsiakas, C.F. Ludwig, F. T. Beil, J.M. Pestka, M. Hahn, R. Santer, C. Supanchart, U. Kornak, A. Del Fattore, T.J. Jentsch, A. Teti, A. Schulz, T. Schinke, M. Amling, CLCN7 and TCIRG1 mutations differentially affect bone matrix mineralization in osteopetrotic individuals, J. Bone Miner. Res. 29 (4) (2014 Apr) 982–991.
[62] E. Palagano, H.C. Blair, A. Pangrazio, I. Tourkova, D. Strina, A. Angius, G. Cuccuru, M. Oppo, P. Uva, W. Van Hul, E. Boudin, A. Superti-Furga, F. Faletra, A. Nocerino, M.C. Ferrari, G. Grappiolo, M. Monari, A. Montanelli, P. Vezzoni, A. Villa, C. Sobacchi, Buried in the middle but guilty: intronic mutations in the TCIRG1 gene cause human autosomal recessive osteopetrosis, J. Bone Miner. Res. 30 (10) (2015 Oct) 1814–1821.
[63] W. Xing, J. Liu, S. Cheng, P. Vogel, S. Mohan, R. Brommage, Targeted disruption of leucine-rich repeat kinase 1 but not leucine-rich repeat kinase 2 in mice causes severe osteopetrosis, J. Bone Miner. Res. 28 (2013) 1962–1974.
[64] J.D. Young, S.Y. Yao, J.M. Baldwin, C.E. Cass, S.A. Baldwin, The human concentrative and equilibrative nucleoside transporter families, SLC28 and SLC29, Mol. Asp. Med. 34 (2013) 529–547.
[65] N. Kang, A.H. Jun, Y.D. Bhutia, N. Kannan, J.D. Unadkat, R. Govindarajan, Human equilibrative nucleoside transporter-3 (hENT3) spectrum disorder mutations impair nucleoside transport, protein localization, and stability, J. Biol. Chem. 285 (36) (2010 Sep 3) 28343–28352.
[66] S.A. Baldwin, S.Y. Yao, R.J. Hyde, A.M. Ng, S. Foppolo, K. Barnes, M.W. Ritzel, C. E. Cass, J.D. Young, Functional characterization of novel human and mouse equilibrative nucleoside transporters (hENT3 and mENT3) located in intracellular membranes, J. Biol. Chem. 280 (16) (2005 Apr 22) 15880–15887.
[67] R. Govindarajan, G.P. Leung, M. Zhou, C.M. Tse, J. Wang, J.D. Unadkat, Facilitated mitochondrial import of antiviral and anticancer nucleoside drugs by human equilibrative nucleoside transporter-3, Am. J. Physiol. Gastrointest. Liver Physiol. 296 (4) (2009 Apr) G910–G922.
[68] N.V. Morgan, M.R. Morris, H. Cangul, D. Gleeson, A. Straatman-Iwanowska, N. Davies, S. Keenan, S. Pasha, F. Rahman, D. Gentle, M.P. Vreeswijk, P. Devilee, M.A. Knowles, S. Ceylaner, R.C. Trembath, C. Dalence, E. Kismet, V. Köseoğlu, H. C. Rossbach, P. Gissen, D. Tannahill, E.R. Maher, Mutations in SLC29A3, encoding an equilibrative nucleoside transporter ENT3, cause a familial histiocytosis syndrome (Faisalabad histiocytosis) and familial rosai-dorfman disease, PLoS Genet. 6 (2) (2010 Feb 5), e1000833.
[69] M.F. Rahman, C. Askwith, R. Govindarajan, Molecular determinants of acidic pH-dependent transport of human equilibrative nucleoside transporter 3, J. Biol. Chem. 292 (36) (2017 Sep 8) 14775–14785.
[70] A. Singh, R. Govindarajan, ENT3 utilizes a pH sensing mechanism for transport, Channels (Austin) 12 (1) (2018 Jan 1) 78–80.
[71] A. Bolze, A. Abhyankar, A.V. Grant, B. Patel, R. Yadav, M. Byun, D. Caillez, J. F. Emile, M. Pastor-Anglada, L. Abel, A. Puel, R. Govindarajan, L. de Pontual, J. L. Casanova, A mild form of SLC29A3 disorder: a frameshift deletion leads to the paradoxical translation of an otherwise noncoding mRNA splice variant, PLoS One 7 (1) (2012), e29708.
[72] M. Farooq, R.M. Moustafa, A. Fujimoto, H. Fujikawa, O. Abbas, A.G. Kibbi, M. Kurban, Y. Shimomura, Identification of two novel mutations in SLC29A3 encoding an equilibrative nucleoside transporter (hENT3) in two distinct Syrian families with H syndrome: expression studies of SLC29A3 (hENT3) in human skin, Dermatology 224 (3) (2012) 277–284.
[73] S.T. Cliffe, J.M. Kramer, K. Hussain, J.H. Robben, E.K. de Jong, A.P. de Brouwer, E. Nibbeling, E.J. Kamsteeg, M. Wong, J. Prendiville, C. James, R. Padidela, C. Becknell, H. van Bokhoven, P.M. Deen, R.C. Hennekam, R. Lindeman, A. Schenck, T. Roscioli, M.F. Buckley, SLC29A3 gene is mutated in pigmented hypertrichosis with insulin-dependent diabetes mellitus syndrome and interacts with the insulin signaling pathway, Hum. Mol. Genet. 18 (12) (2009 Jun 15) 2257–2265.
[74] C.L. Hsu, W. Lin, D. Seshasayee, Y.H. Chen, X. Ding, Z. Lin, E. Suto, Z. Huang, W. P. Lee, H. Park, M. Xu, M. Sun, L. Rangell, J.L. Lutman, S. Ulufatu, E. Stefanich, C. Chalouni, M. Sagolla, L. Diehl, P. Fielder, B. Dean, M. Balazs, F. Martin, Equilibrative nucleoside transporter 3 deficiency perturbs lysosome function and macrophage homeostasis, Science 335 (6064) (2012 Jan 6) 89–92.
[75] S. Nair, A.M. Strohecker, A.K. Persaud, B. Bissa, S. Murugananden, C. McElroy, R. Pathak, M. Williams, R. Raj, A. Kaddoumi, A. Sparreboom, A.M. Beedle, R. Govindarajan, Adult stem cell deficits drive Slc29a3 disorders in mice, Nat. Commun. 10 (1) (2019 Jul 3) 2943.
[76] B. Biteau, C.E. Hochmuth, H. Jasper, Maintaining tissue homeostasis: dynamic control of somatic stem cell activity, Cell Stem Cell 9 (2011) 402–411.
[77] A. Hampe, B.M. Shamoon, M. Gobet, C.J. Sherr, F. Galibert, Nucleotide sequence and structural organization of the human FMS proto-oncogene, Oncogene Res. 4 (1) (1989) 9–17. PMID: 2524025.
[78] S.A. Ridge, M. Worwood, D. Oscier, A. Jacobs, R.A. Padua, FMS mutations in myelodysplastic, leukemic, and normal subjects, Proc. Natl. Acad. Sci. U. S. A. 87 (4) (1990 Feb) 1377–1380.
[79] P.V. Byrne, L.J. Guilbert, E.R. Stanley, Distribution of cells bearing receptors for a colony-stimulating factor (CSF-1) in murine tissues, J. Cell Biol. 91 (3 Pt 1) (1981 Dec) 848–853.
[80] S.R. Himes, D.P. Sester, T. Ravasi, S.L. Cronau, T. Sasmono, D.A. Hume, The JNK are important for development and survival of macrophages, J. Immunol. 176 (4) (2006 Feb 15) 2219–2228.
[81] C. Svensson, K. Part, K. Künnis-Beres, M. Kaldmäe, S.Z. Fernaeus, T. Land, Pro-survival effects of JNK and p38 MAPK pathways in LPS-induced activation of BV-2 cells, Biochem. Biophys. Res. Commun. 406 (3) (2011 Mar 18) 488–492.
[82] R. Rademakers, M. Baker, A.M. Nicholson, N.J. Rutherford, N. Finch, A. Soto-Ortolaza, J. Lash, C. Wider, A. Wojtas, M. DeJesus-Hernandez, J. Adamson, N. Kouri, C. Sundal, E.A. Shuster, J. Aasly, J. MacKenzie, S. Roeber, H. A. Kretzschmar, B.F. Boeve, D.S. Knopman, R.C. Petersen, N.J. Cairns, B. Ghetti, S. Spina, J. Garbern, A.C. Tselis, R. Uitti, P. Das, J.A. Van Gerpen, J.F. Meschia, S. Levy, D.F. Broderick, N. Graff-Radford, O.A. Ross, B.B. Miller, R.H. Swerdlow, D. W. Dickson, Z.K. Wszolek, Mutations in the colony stimulating factor 1 receptor (CSF1R) gene cause hereditary diffuse leukoencephalopathy with spheroids, Nat. Genet. 44 (2) (2011 Dec 25) 200–205.
[83] B. Erblich, L. Zhu, A.M. Etgen, K. Dobrenis, J.W. Pollard, Absence of colony stimulation factor-1 receptor results in loss of microglia, disrupted brain development and olfactory deficits, PLoS One 6 (10) (2011), e26317.
[84] P.M. Tamhankar, B. Zhu, V.P. Tamhankar, S. Mithbawkar, L. Seabra, J. H. Livingston, T. Ikeuchi, Y.J. Crow, A novel hypomorphic CSF1R gene mutation in the biallelic state leading to fatal childhood neurodegeneration, Neuropediatrics 51 (4) (2020 Aug) 302–306.
[85] V. Chitu, Ş. Gökhan, E.R. Stanley, Modeling CSF-1 receptor deficiency diseases - how close are we? FEBS J. (2021 Jun 19) https://doi.org/10.1111/febs.16085.
[86] V. Chitu, S. Gokhan, M. Gulinello, C.A. Branch, M. Patil, R. Basu, C. Stoddart, M. F. Mehler, E.R. Stanley, Phenotypic characterization of a Csf1r haploinsufficient mouse model of adult-onset leukodystrophy with axonal spheroids and pigmented glia (ALSP), Neurobiol. Dis. 74 (2015 Feb) 219–228.
[87] T. Konno, M. Tada, M. Tada, A. Koyama, H. Nozaki, Y. Harigaya, J. Nishimiya, A. Matsunaga, N. Yoshikura, K. Ishihara, M. Arakawa, A. Isami, K. Okazaki, H. Yokoo, K. Itoh, M. Yoneda, M. Kawamura, T. Inuzuka, H. Takahashi, M. Nishizawa, O. Onodera, A. Kakita, T. Ikeuchi, Haploinsufficiency of CSF-1R and clinicopathologic characterization in patients with HDLS, Neurology 82 (2) (2014 Jan 14) 139–148.
[88] O.L. Patkar, M. Caruso, N. Teakle, S. Keshvari, S.J. Bush, C. Pridans, A. Belmer, K. M. Summers, K.M. Irvine, D.A. Hume, Analysis of homozygous and heterozygous Csf1r knockout in the rat as a model for understanding microglial function in brain development and the impacts of human CSF1R mutations, Neurobiol. Dis. 151 (2021 Apr), 105268.
[89] D. Korr, L. Toschi, P. Donner, H.D. Pohlenz, B. Kreft, B. Weiss, LRRK1 protein kinase activity is stimulated upon binding of GTP to its roc domain, Cell. Signal. 18 (6) (2006 Jun) 910–920.
[90] J.N. Harada, K.E. Bower, A.P. Orth, S. Callaway, C.G. Nelson, C. Laris, J. B. Hogenesch, P.K. Vogt, S.K. Chanda, Identification of novel mammalian growth regulatory factors by genome-scale quantitative image analysis, Genome Res. 15 (8) (2005 Aug) 1136–1144.
[91] W.R. Xing, H. Goodluck, C. Zeng, S. Mohan, Role and mechanism of action of leucine-rich repeat kinase 1 in bone, Bone Res. 14 (5) (2017 Mar) 17003.
[92] M. Si, H. Goodluck, C. Zeng, S. Pan, E.M. Todd, S.C. Morley, X. Qin, S. Mohan, W. Xing, LRRK1 regulation of actin assembly in osteoclasts involves serine 5 phosphorylation of L-plastin, J. Cell. Biochem. 119 (12) (2018 Dec) 10351–10357.
[93] K.P. McHugh, K. Hodivala-Dilke, M.H. Zheng, N. Namba, J. Lam, D. Novack, X. Feng, F.P. Ross, R.O. Hynes, S.L. Teitelbaum, Mice lacking beta3 integrins are osteosclerotic because of dysfunctional osteoclasts, J. Clin. Invest. 105 (4) (2000 Feb) 433–440.

[94] M. Croke, F.P. Ross, M. Korhonen, D.A. Williams, W. Zou, S.L. Teitelbaum, Rac deletion in osteoclasts causes severe osteopetrosis, J. Cell Sci. 124 (Pt 22) (2011 Nov 15) 3811–3821.
[95] M. Zhu, B.H. Sun, K. Saar, C. Simpson, N. Troiano, S.L. Dallas, L.M. Tiede-Lewis, E. Nevius, J.P. Pereira, R.S. Weinstein, S.M. Tommasini, K.L. Insogna, Deletion of rac in mature osteoclasts causes osteopetrosis, an age-dependent change in osteoclast number, and a reduced number of osteoblasts in vivo, J. Bone Miner. Res. 31 (4) (2016 Apr) 864–873.
[96] Y. Xu, X. Yu, M. Huang, A novel mutation in TNFRSF11A gene causes pediatric osteopetrosis: case report, BMC Surg. 21 (1) (2021 May 28) 269.
[97] P. Lertwilaiwittaya, B. Suktitipat, P. Khongthon, W. Pongsapich, C. Limwongse, M. Pithukpakorn, Identification of novel mutation in RANKL by whole-exome sequencing in a Thai family with osteopetrosis; a case report and review of RANKL osteopetrosis, Mol. Genet. Genomic Med. 9 (7) (2021 Jul), e1727.